

Late Mesozoic intracontinental reactivation of the southern Altai, Central Asia

Zhiyuan He^{1,†}, Shida Song¹, Fujun Wang², Wenbin Zhu^{2,†}, Xiaoming Shen³, Stijn Glorie⁴, Yong Liang¹, Linglin Zhong⁵, and Johan De Grave¹

¹Laboratory for Mineralogy and Petrology, Department of Geology, Ghent University, Krijgslaan 281 S8, 9000 Ghent, Belgium

²State Key Laboratory for Mineral Deposits Research, School of Earth Sciences and Engineering, Nanjing University, 210023 Nanjing, China

³National Institute of Natural Hazards, Ministry of Emergency Management of China, Beijing 100085, China

⁴Department of Earth Sciences, School of Physical Sciences, The University of Adelaide, South Australia 5005, Australia

⁵College of Earth Sciences, Chengdu University of Technology, Chengdu 610059, Sichuan, China

ABSTRACT

The Altai orogenic belt is a main constituent of the Central Asian Orogenic Belt, and serves as a crucial site for studying strain propagation from the Meso-Cenozoic plate margins to the Eurasian interior. The ranges of the Altai Mountains have undergone multiple reactivation events during the Mesozoic and Cenozoic, but the full extent of these events is not yet fully understood. To constrain the thermo-tectonic history of the southern Altai orogenic belt of Northwest China, apatite fission-track (AFT) and apatite (U-Th)/He (AHe) thermochronological methods were used to study 29 pre-Mesozoic basement rocks from several key localities, including the Altay, Xibodu, Fuyun, and Qinghe regions. Late Jurassic to Early Cretaceous AFT and AHe ages were found in the low-elevation Xibodu region, which has been characterized by slow-to-moderate rock cooling since the Jurassic. However, rock samples from all other regions investigated are characterized by comparable Late Cretaceous AFT and AHe ages. Inverse thermal history modeling results reveal moderate-to-rapid upper crustal cooling in the mid- to Late Cretaceous (ca. 110–70 Ma), which is interpreted to be related to distant plate-margin processes (e.g., the Cimmerian collisions). These findings, combined with previously published data, indicate that Late Cretaceous exhumation was widespread in the western Altai orogenic belt, including in the Chinese and Sibe-

rian (Russian) parts of the Altai region. As in many other areas of Central Asia, no Cenozoic low-temperature thermochronological signal was detected in this study. We propose that Cenozoic deformation indeed occurred in the southern Altai, but the magnitude of associated denudation was insufficient to have replaced the Cretaceous cooling signals.

INTRODUCTION

Throughout Earth's history, the interactions among lithospheric plates have been a principal mechanism sculpting the geological evolution of our planet's surface. While the bulk of deformation and tectonic activity is predominantly manifested at plate margins, discernible deformation also transpires within continental interiors. This phenomenon, commonly referred to as intracontinental deformation, is posited to arise from stress transfer mechanisms originating from far-field forces generated at plate margins and subsequently propagated through the lithosphere (e.g., Cunningham, 2005; De Grave et al., 2007; Raimondo et al., 2014). Unraveling the complexities surrounding the evolution and dynamics of intracontinental tectonic deformation, and its complicated interplay with surface processes and climate, constitute a challenge (Burbank and Pinter, 1999; Whipple, 2009; Morin et al., 2018). In general, stress transport through the lithosphere is thought to be an important mechanism for large-scale intracontinental deformation. Forces from distant plate margins are partitioned into the continental interior, which affects the weaker and more mobile parts of the intracontinental structural fabrics (Holdsworth et al., 1997; Cunningham, 2010; Glorie, 2012). Typically, the correlation between plate margin processes and the incidence of compressive intracontinental

deformation has been scrutinized within the reactivated segments of the Central Asian Orogenic Belt, in which the continental interior has undergone active deformation primarily in response to the multiple accretion-collision events taking place along the Eurasian margins (Avouac and Tapponnier, 1993; Glorie et al., 2010; Jolivet et al., 2013; Käßner et al., 2017).

The Central Asian Orogenic Belt is the most expansive Phanerozoic accretionary orogenic belt. It spans the territory between the Baltica and Siberian cratons to the north, and the Tarim and North China cratons to the south (Jahn, 2004; Windley et al., 2007). It also preserves important phases of continental growth from the Neoproterozoic to Early Triassic and is exposed in the southwestern, reactivated part of the belt where, nowadays, a large intracontinental deformation zone exists, pinched between the North China and Tarim cratons, Kazakhstan, and Siberia (Fig. 1A). Extending from the Pamir region in the southwest to the Baikal rift in the northeast, this deformation zone mainly traverses the ranges of the Tianshan, Junggar, Altai, and Sayan mountains (Fig. 1A; Glorie and De Grave, 2016). The present-day intracontinental deformation occurring in these regions is, to a large extent, interpreted as the far-field response of India-Eurasia collision, which demonstrates that plate margin processes can spectacularly affect the continental interiors far from the plate margins (Tapponnier and Molnar, 1979; Sobel et al., 2006a). In an analogue manner, parts of the Central Asian Orogenic Belt have been reactivated episodically throughout geological history. The spatio-temporal extent of these reactivation episodes and their causative mechanisms are often difficult to reconstruct due to uncertainties regarding the timing and nature of the plate margin processes, the delayed response in the continental interior and

Zhiyuan He  <https://orcid.org/0000-0002-5169-5557>

[†]Z. He, RonnieHo1993@gmail.com; W. Zhu, zwb@nju.edu.cn

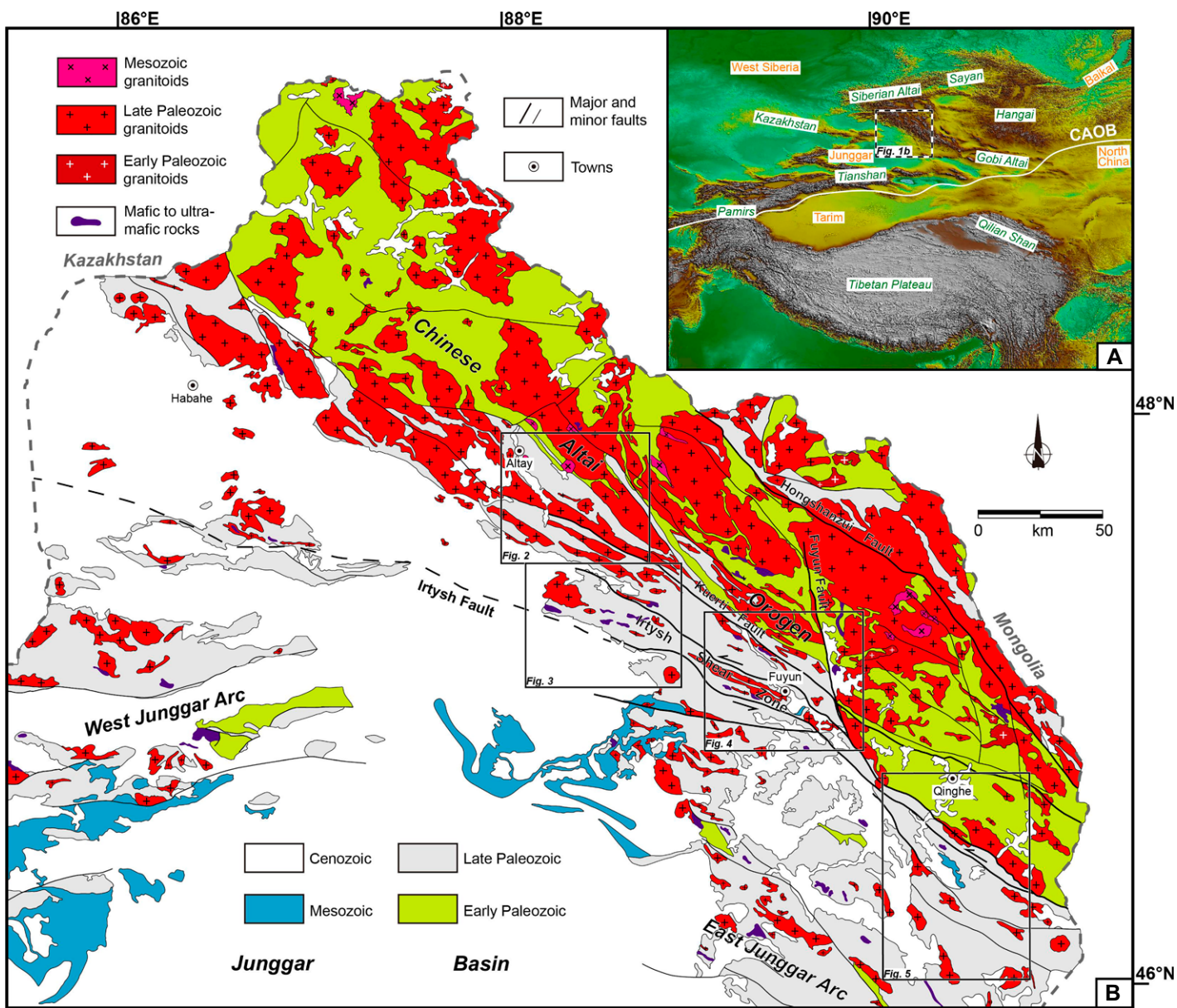


Figure 1. (A) Topographic overview map of Central Asia, with the main mountain ranges and basins labeled. (B) Simplified geological map of the southern (Chinese) Altai and its neighboring tectonic units, with major structures shown (based on XBGMR, 1993). Black boxes indicate the study areas. CAOB—Central Asian orogenic belt.

interactions between tectonics and surface processes, and the possible overprint by more recent deformation (Jolivet et al., 2010; De Grave et al., 2014; Glorie and De Grave, 2016; He, 2022).

The Altai orogen is situated between the Sayan and associated terranes to the north and the Kazakhstan-Junggar terrane to the south, and it represents a major segment of the middle Central Asian Orogenic Belt (Fig. 1). The orogen geographically extends southward from the Rudny Altai in Siberia, via the Altai of western Mongolia, to the Chinese Altai, where the highest mountains of the Altai ranges (the Tavan Bogd in Mongolia, with an elevation of ~4374 m) are located

(De Grave et al., 2008). Like the Tianshan orogenic belt to the south, Mesozoic reactivation and denudation in the Altai have been documented based on low-temperature thermochronology (e.g., De Grave and Van den Haute, 2002; Glorie et al., 2012a). Thus far, the southern part of the Altai orogen (largely located in Chinese territory) has been extensively studied for its Paleozoic accretionary and collisional events, but limited attention has been paid to its Mesozoic–Cenozoic reactivation history (Yuan et al., 2006; Glorie et al., 2023). This area is structurally dominated by the vast Irtysh shear zone and several subordinate ~NW–SE-striking brittle faults, which

were crosscut by the ~N–S dextral Fuyun fault (Fig. 1B). The reactivation and intracontinental deformation histories of these structures remain poorly understood and require further investigation, so a comparison to the thermo-tectonic history of the well-studied Siberian-Mongolian Altai in the north (e.g., Glorie et al., 2012a; De Grave et al., 2014) is necessary. This study presents new apatite fission-track (AFT) and apatite (U-Th)/He (AHe) age data for 29 Paleozoic igneous and metasedimentary rock samples collected from a broad area of the southern Altai orogen. We combine the thermochronologically derived exhumation histories and available thermochro-

nological constraints to examine the magnitude of intracontinental deformation across the entire Altai orogen since the Mesozoic.

GEOLOGICAL BACKGROUND

Basement History

The southern Altai (Chinese part) is characterized by Paleozoic and early Mesozoic basement

rocks, which include extensive metasedimentary rocks and voluminous granitoids (Fig. 1B). Cambrian to Silurian strata are the oldest sedimentary sequences in the southern Altai, mainly comprising sandstone, siltstone, and shale that have largely experienced regional metamorphism (Windley et al., 2002; Long et al., 2007). Detrital zircon U-Pb dating results of these metasedimentary rocks show prominent zircon age populations of between ca. 550 Ma and

ca. 460 Ma, with inherited Precambrian grains (Long et al., 2007; Jiang et al., 2011). The Devonian strata are composed of the Kangbutiebao and Altay formations that crop out discontinuously in the depositional basins of the study area, distributed from the NW to SE (Figs. 2 and 3). The former is a suite of volcanic and pyroclastic rocks that experienced greenschist- to lower amphibolite-facies metamorphism. Zircons from metarhyolites of this formation yielded U-Pb

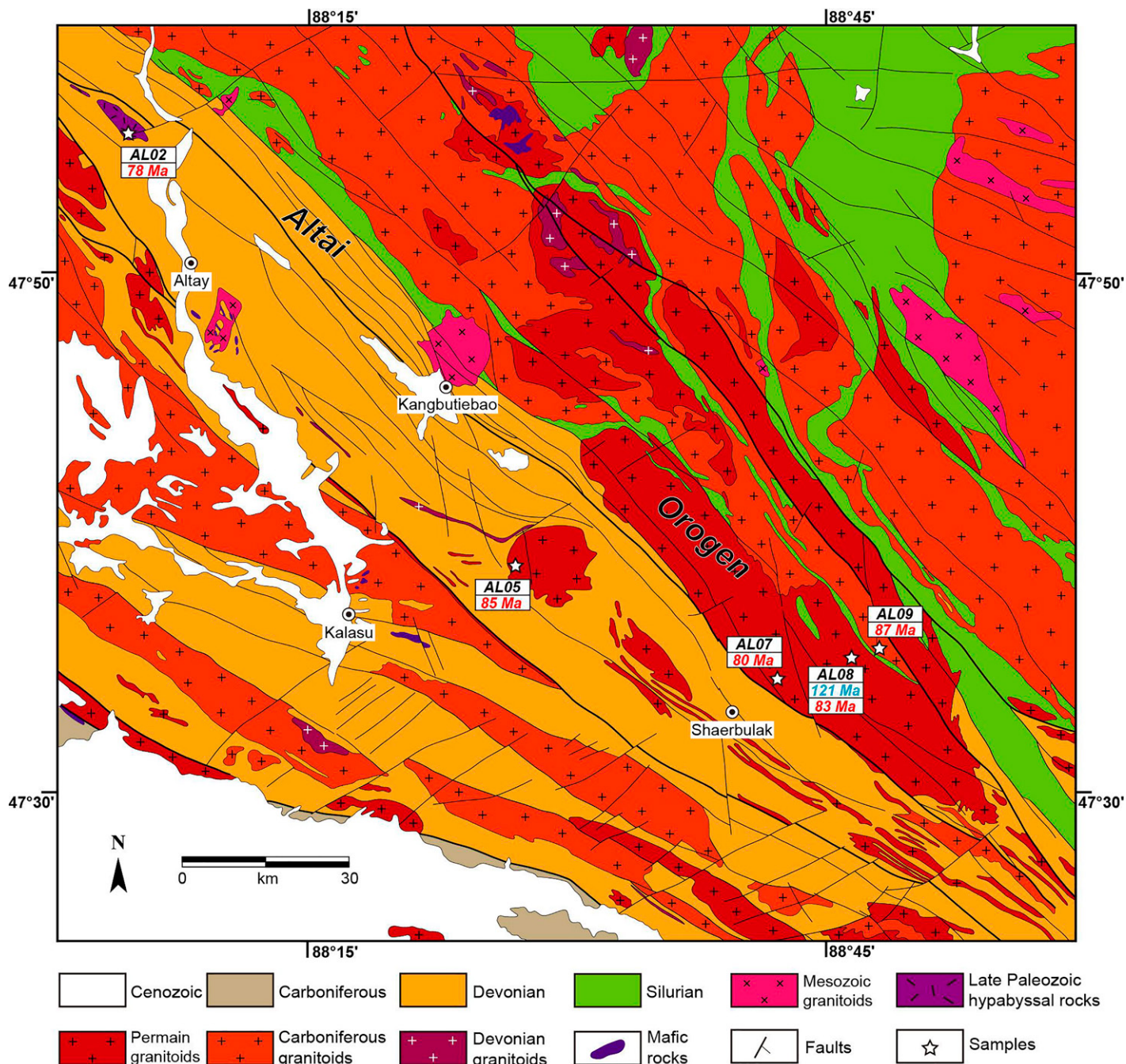


Figure 2. Simplified geological map of the Altai region, Central Asia (based on XBGMR, 1978a). Locations of sample sites and the newly obtained apatite fission-track (in red font) and apatite (U-Th)/He (in blue font) ages are indicated.

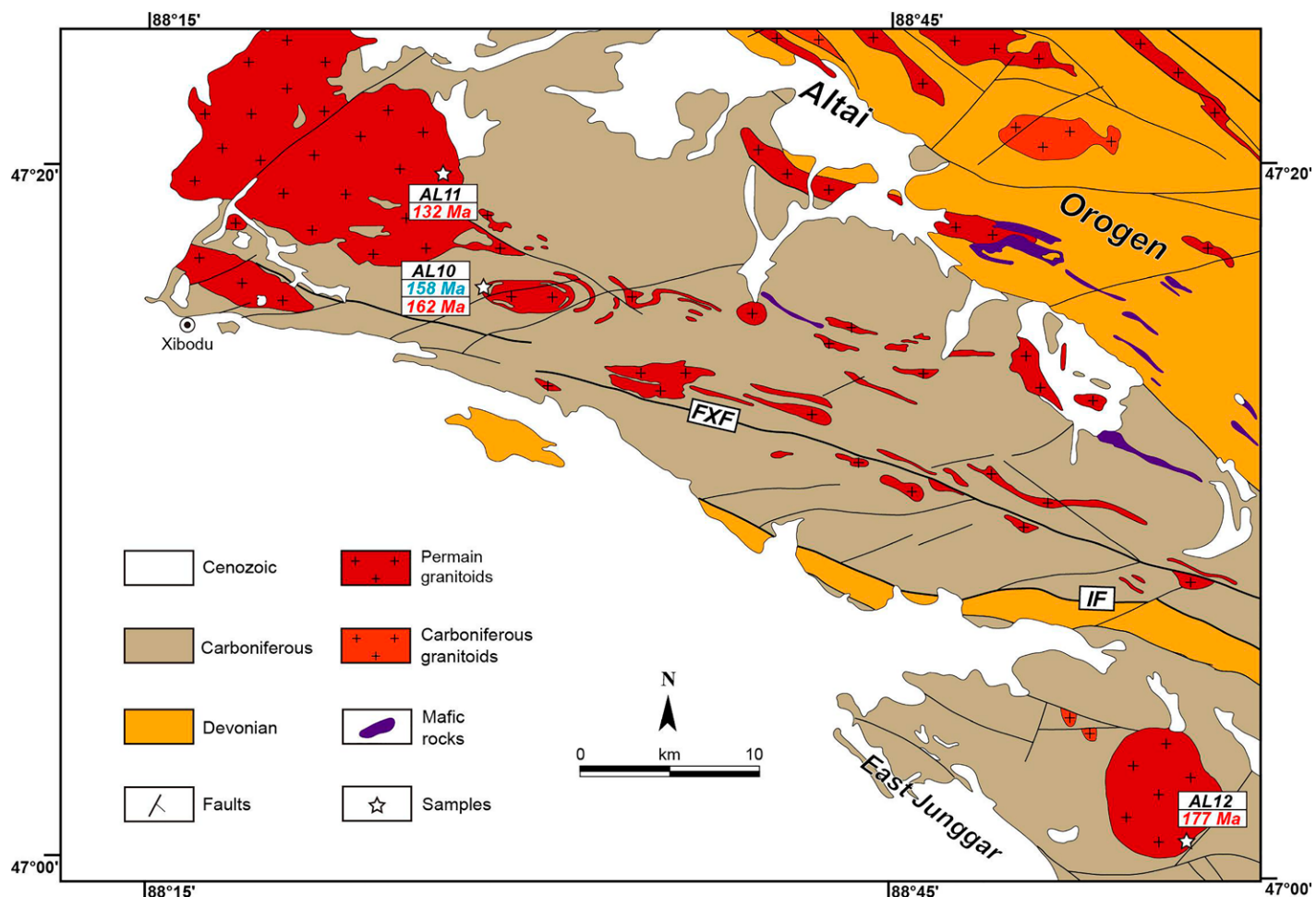


Figure 3. Simplified geological map of the Xibodu region, Central Asia (based on XBGM, 1978b). Locations of sample sites, and the newly obtained apatite fission-track (in red font) and apatite (U-Th)/He (in blue font) ages are indicated. FXF—Fuyun-Xibodu fault; IF—Irtysk fault.

ages of ca. 412–400 Ma (Chai et al., 2009; Liu et al., 2010). The Altay Formation is composed of marine clastic rocks and minor pillow basalts, and is mainly distributed along the Habahe–Altay–Fuyun regions (Fig. 1B; Windley et al., 2002). The youngest stratigraphic sequences in the southern Altai are Carboniferous strata, which mainly consist of slate, siltstone, schist, and amphibolite-facies gneiss (Windley et al., 2002; Liu et al., 2012). Its maximum depositional age was constrained to ca. 326–322 Ma, based on the youngest zircon U-Pb age populations of the schist samples from the Irtysh shear zone (Li et al., 2015b).

The southern Altai recorded prolonged and extensive granitic magmatism from the Cambrian to Triassic, with most of the granitoids being of Paleozoic age (Fig. 1B). Cai et al. (2011) found that plutonism in the southern Altai was continuous in the early to mid-Paleozoic, while its activity decreased significantly in the late Paleozoic and early Mesozoic, when it was weak and had only limited distribution. The early to mid-Paleo-

zoic granitoids mainly include both I- and S-type tonalites, granodiorites, and granites, most with distinct arc-like geochemical signatures (e.g., Sun et al., 2008; Cai et al., 2011; Kong et al., 2019). Published zircon U-Pb ages reveal that the crystallization of these granitoids occurred between ca. 507 Ma and ca. 360 Ma, with peak activity at ca. 400 Ma. The latest emplacement of the subduction-related granites occurred at ca. 330–313 Ma (Chen and Jahn, 2002; Cai et al., 2012). The magma sources of the Cambrian to Carboniferous granitoids are thought to be intermediate to mafic mid-lower crustal rocks or immature sedimentary rocks, based on whole-rock geochemistry and pseudosection modeling (Yuan et al., 2007; Jiang et al., 2016). The latest Carboniferous to Permian granites intruded the southern Altai basement between ca. 311 Ma and ca. 252 Ma, and mainly include K-feldspar and biotite granite and monzogranite (Zhang et al., 2012; Tong et al., 2014). Among these, A-type granitic bodies of alkali-feldspar granites have crystallization ages younger than ca. 300 Ma,

and have been interpreted as post-orogenic granitoids (e.g., Tong et al., 2006; Shen et al., 2011). The Triassic granites (ca. 220–198 Ma) are only sparsely distributed in the southern Altai. They are mainly composed of biotite granite, monzogranite, and pegmatite that were formed in an intraplate anorogenic setting (Wang et al., 2009; Lin et al., 2019).

Structural Architecture

The southern Altai was structurally affected by large-scale transcurrent motion along the Irtysh shear zone, which is a major suture that represents the tectonic boundary between the southern margin of the peri-Siberian orogenic system (i.e., the Chinese Altai orogen) and the East and West Junggar arcs (Fig. 1B; Laurent-Charvet et al., 2003; Li et al., 2017). Previous structural mapping revealed that this shear zone features a series of fold zones bounded by mylonitic zones and was subjected to three phases of folding and shear deformation (within

a time span of \sim 322–252 m.y.) in the late Paleozoic, including a main sinistral motion (e.g., Li et al., 2015b, 2016). Available biotite and muscovite $^{40}\text{Ar}/^{39}\text{Ar}$ data from the Fuyun region indicate that the sinistral movements of the Irtysh shear zone took place during ca. 290–250 Ma (e.g., Laurent-Charvet et al., 2003; Briggs et al., 2007). In the eastern segment of the Irtysh shear zone, structural observations and mica $^{40}\text{Ar}/^{39}\text{Ar}$

dating results from the Qinghe region show four NW–SE sinistral mylonitic zones that were active between ca. 283 Ma and ca. 265 Ma. Areas in between these mylonitic zones exhibit variable fold patterns (Hu et al., 2020). The southern Altai also exposes a network of strike-slip and thrust faults that have accommodated Cenozoic intraplate crustal shortening in response to India-Asia collision (e.g., the Hongshanzui, Kuerti,

and Fuyun faults). The Fuyun fault is a Cenozoic dextral fault cutting the Irtysh shear zone (Figs. 1B and 4). The Fuyun fault strikes nearly N–S before deviating slightly eastward, and has a total length of >200 km. Recent surficial geological mapping and geodetic investigations have clearly demonstrated its Quaternary right-lateral strike-slip faulting (Klinger et al., 2011; Wu et al., 2024).

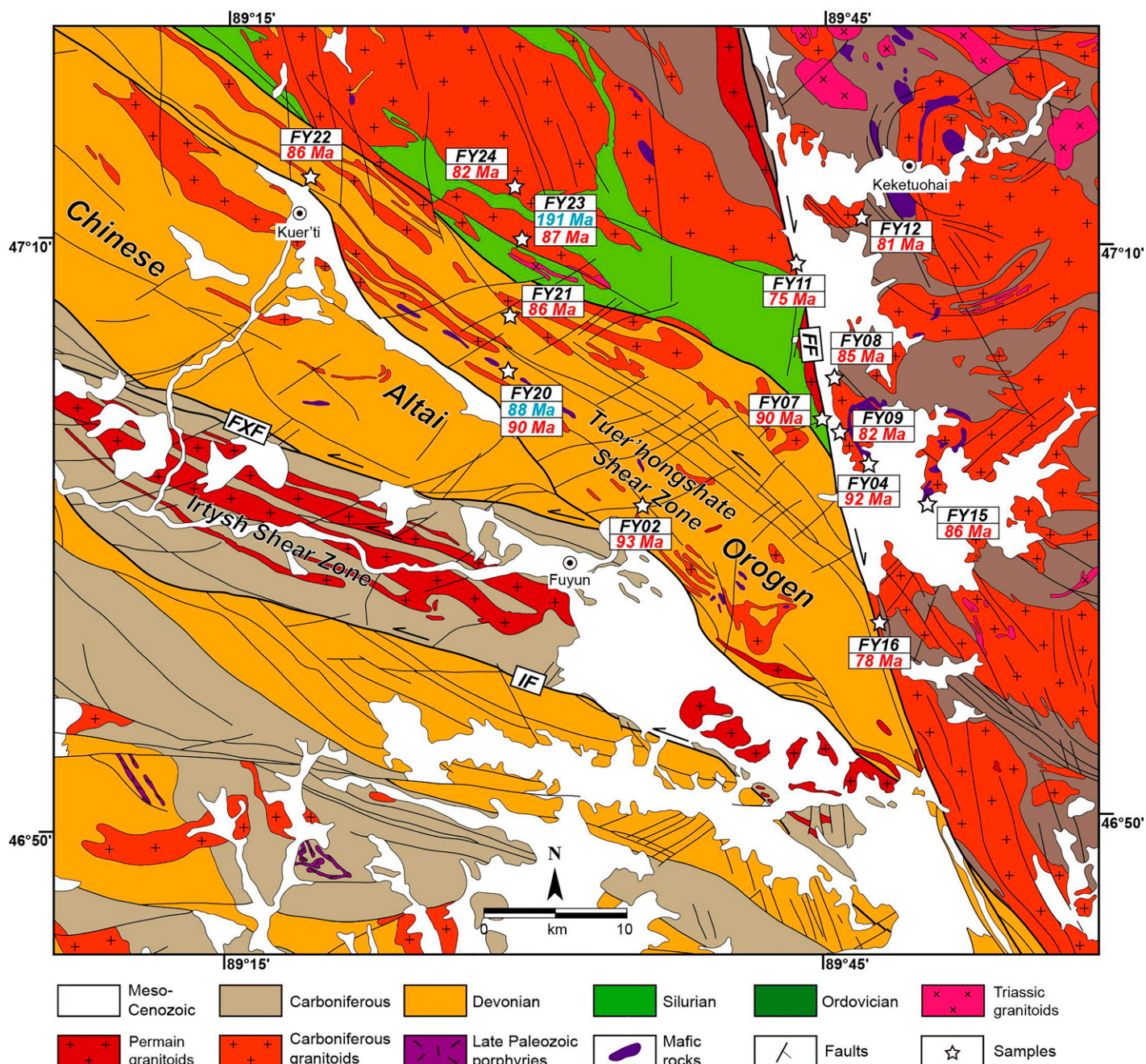


Figure 4. Simplified geological map of the Fuyun region, Central Asia (based on XBGMR, 1978c). Locations of sample sites and the newly obtained apatite fission-track (in red font) and apatite (U-Th)/He (in blue font) ages are indicated. FF—Fuyun fault; FXF—Fuyun-Xibodu fault; IF—Irtysh fault.

SAMPLES AND METHODOLOGY

Sample Sites

A total of 29 pre-Mesozoic basement rocks (igneous bodies or metasedimentary rocks) were collected as widely as possible throughout four

main regions (Fig. 1) in the southern Altai. In the Fuyun and Qinghe areas, attention was paid to major structures, and several samples were taken from distinct fault zones, such as the Irtysh shear zone and Fuyun fault (Figs. 4 and 5). Table 1 provides information about the samples, including lithology, geographical locations, and elevations.

Methods

The main method applied to all samples in this study was AFT analysis. AFT data record the cooling history of the sample through the apatite partial annealing zone ($\sim 120\text{--}60$ °C; e.g., Wagner and Van den Haute, 1992; Donelick

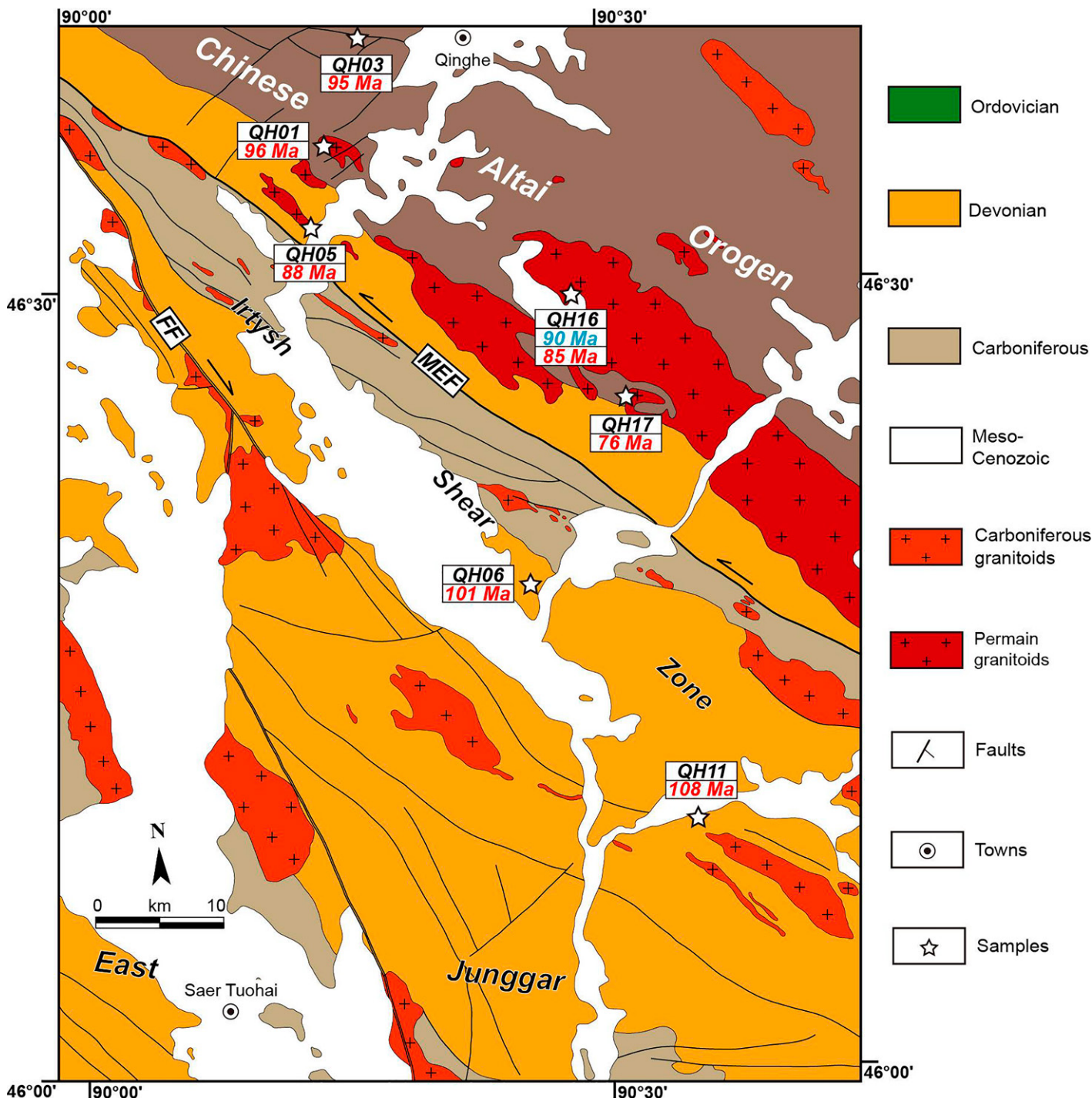


Figure 5. Simplified geological map of the Qinghe region of Central Asia (based on XBGMR, 1965). Locations of sample sites, and the newly obtained apatite fission-track (in red font) and apatite (U-Th)/He (in blue font) ages are indicated. FF—Fuyun fault; MEF—Mayin'erbo fault.

TABLE 1. SUMMARY OF INFORMATION AND THERMOCHRONOLOGICAL RESULTS FOR SAMPLES WITHIN THE SOUTHERN ALTAI OROGEN, CENTRAL ASIA

Sample ID	Lithology	Latitude (°N)	Longitude (°E)	Elevation (m)	AFT central age (Ma)	AHe mean age (Ma)
Altay region						
AL02	Granitic gneiss	47°56'26.48"	88°05'06.27"	1287	77.7 ± 7.8	—
AL05	Granite	47°39'11.41"	88°26'49.62"	832	84.6 ± 3.5	—
AL07	Granite	47°34'35.38"	88°42'18.64"	1109	80.4 ± 3.7	—
AL08	Granitic gneiss	47°35'10.10"	88°46'33.19"	916	82.9 ± 5.8	121.2 ± 3.6
AL09	Granitic gneiss	47°35'32.20"	88°48'37.06"	1137	86.7 ± 3.5	—
Xibodu region						
AL10	Granitic gneiss	47°16'40.86"	88°28'28.28"	715	161.7 ± 8.7	158.4 ± 4.8
AL11	Granite	47°19'46.93"	88°27'04.35"	691	131.8 ± 7.5	—
AL12	Granitic gneiss	47°00'44.30"	88°57'29.57"	785	177.0 ± 13.0	—
Fuyun region						
FY02	Granitic gneiss	47°01'13.53"	89°35'13.80"	796	92.5 ± 3.3	—
FY04	Granitic gneiss	47°02'33.60"	89°47'01.50"	1197	92.3 ± 4.7	—
FY07	Mica schist	47°03'18.59"	89°45'4.85"	1233	90.0 ± 7.7	—
FY08	Granite	47°05'41.56"	89°45'07.20"	1216	84.6 ± 4.4	—
FY09	Granite	47°03'34.11"	89°45'22.78"	1322	82.0 ± 13.0	—
FY11	Granite	47°09'26.18"	89°43'28.75"	1134	74.8 ± 6.0	—
FY12	Granitic gneiss	47°10'59.80"	89°47'01.72"	1233	80.7 ± 3.6	—
FY15	Granite	47°01'11.74"	89°49'37.90"	1303	85.9 ± 6.3	—
FY16	Granitic gneiss	46°57'11.99"	89°47'18.37"	1210	78.2 ± 3.3	—
FY20	Granitic gneiss	47°06'00.04"	89°28'35.25"	1157	89.7 ± 3.1	88.4 ± 2.2
FY21	Granitic gneiss	47°08'02.58"	89°28'35.21"	1369	85.8 ± 3.5	—
FY22	Granitic gneiss	47°12'52.72"	89°18'48.73"	1000	85.7 ± 3.3	—
FY23	Granite	47°10'49.11"	88°29'32.42"	1510	86.5 ± 5.3	191.1 ± 6.2
FY24	Granite	47°12'29.40"	88°29'11.20"	1572	81.8 ± 5.7	—
Qinghe region						
QH01	Granitic gneiss	46°35'19.97"	90°14'30.71"	1266	96.1 ± 3.9	—
QH03	Granitic gneiss	46°40'31.51"	90°17'10.76"	1365	94.7 ± 4.7	—
QH05	Granitic gneiss	46°31'53.18"	90°14'25.85"	1120	87.9 ± 4.4	—
QH06	Meta-sandstone	46°18'29.40"	90°25'23.53"	1090	101.0 ± 31.0	—
QH11	Meta-sandstone	46°09'40.60"	90°33'42.03"	1097	108.0 ± 43.0	—
QH16	Granitic gneiss	46°29'36.93"	90°27'56.18"	1402	85.1 ± 4.6	89.8 ± 1.9
QH17	Granite	46°25'48.89"	90°30'56.64"	1303	75.6 ± 5.8	—

Note: AFT—apatite fission track; AHe—apatite (U-Th)/He.

et al., 2005). In addition, the AHe dating method was applied to complement the AFT method, as it has a lower closure temperature (~75 °C for complete He retention) and a partial retention zone of 40–80 °C, providing insights into cooler thermal events (Wolf et al., 1998; Ehlers and Farley, 2003). In this study, five granitoid samples were analyzed by AHe dating at the National Institute of Natural Hazards, Ministry of Emergency Management of China, following standard procedures (e.g., Shen et al., 2019; He et al., 2023a). Detailed sample preparation and dating protocols are presented in the Supplemental Material.¹

¹Supplemental Material. Supplemental Text S1: Analytical procedures for thermochronology; Table S1: Apatite fission-track data for Paleozoic basement rocks from the southern Altai; Table S2: Single-grain apatite (U-Th)/He results from the southern Altai; Figure S1: Apatite fission-track radial plots; Figure S2: Apatite (U-Th)/He ages versus effective uranium content (eU); Figure S3: Thermal history modeling results for each analyzed sample generated by QTQt, along with apatite fission-track length distribution histograms for each analyzed sample. Please visit <https://doi.org/10.1130/GSAB.S.27942183> to access the supplemental material; contact editing@geosociety.org with any questions.

To better reconstruct the cooling and exhumation history of the Chinese Altai, we performed thermal history modeling using the QTQt software package (Gallagher, 2012). This software performs inverse thermal modeling based on a transdimensional Bayesian Markov Chain Monte Carlo approach (Gallagher et al., 2009; Gallagher, 2012). Thermal history modeling was conducted on 23 samples that yielded adequate (all >48, mostly ≥100) confined track length measurements. We used the multikinetic fission-track annealing model of Ketcham et al. (2007), with D_{par} serving as the kinetic parameter. For samples that yielded meaningful AHe dates (i.e., AL10, FY20, and QH16), we employed apatite's radiation damage models of He diffusion in the modeling approach (Flowers et al., 2009). In the modeling strategy, the prior for temperature was set as time = central age ± central age, temperature = 70 ± 70 °C. Since all samples were taken from outcrops, the present-day temperature was constrained to 10 ± 10 °C, which seems realistic for current conditions in the study area. For each sample, we first ran the algorithm for 10,000 burn-in and 50,000 post-burn-in iterations to find the appropriate search parameters, and after that 50,000 burn-in and 200,000 post-burn-in iter-

tions were performed for the modeling to obtain a stable result.

ANALYTICAL RESULTS

AFT Data

The AFT results for 29 Paleozoic basement rock samples from the Chinese Altai orogen are summarized in Table 1 and detailed in Table S1 and Figures S1 and S2 include radial plots of single-grain ages and confined AFT length distributions. Up to 20 apatite grains were analyzed per individual sample. However, for two samples (QH06 and QH11), fewer than 10 measurable grains could be extracted. The AFT central ages obtained are predominantly late Mesozoic and range from ca. 177 Ma to ca. 75 Ma, with the majority of samples yielding Late Cretaceous central AFT ages. More specifically, samples from the Altay and Fuyun regions all exhibit comparable Late Cretaceous AFT ages, which cluster at ca. 93–75 Ma (Figs. 2 and 4; Table 1). The central ages of seven samples from the Qinghe region fall in a wider span, from ca. 108 Ma to ca. 76 Ma (Fig. 5; Table 1). In the Xibodu region of the southernmost Altai (Fig. 3), samples AL10–AL12 exhibit the oldest AFT central ages of ca. 177–132 Ma. All samples passed the chi-squared test at the 95% confidence level, which is indicative of a single population of grains (Fig. S1; Table S1; Galbraith and Green, 1990). A minimum of 50 confined tracks could be measured for 22 out of 29 samples, and 100 for 20 samples (Table S1). The mean track lengths for all samples vary between 14 μm and 13 μm, and they show a moderate degree of shortening (compared to the original length) with a unimodal distribution. This suggests that the rocks analyzed have been subjected to limited partial annealing of apatite fission tracks (e.g., Carlson et al., 1999).

Apatite (U-Th)/He Data

A total of 22 single-grain aliquots were analyzed from five samples for AHe thermochronology. The single-grain ages obtained show high dispersion and are frequently older than the corresponding AFT ages (Table S2). A series of factors can result in intrasample variability (i.e., a wide age range), including U-Th zonation, grain fragmentation, radiation damage, and the presence of microinclusions (e.g., Fitzgerald et al., 2006; Brown et al., 2013). Considering these factors, we tried to select only the purest euhedral apatite crystals. Single-grain ages show an excessive lack of correlation of scatter with effective uranium content (Fig. S2), and thus, neither grain fracture nor radiation damage

seemed to be the artifact leading to an overestimation of the age (e.g., Guenthner et al., 2013). In this case, the overdispersion of the AHe dates is more likely due to helium implantation, considering the low eU contents (<15–20 ppm) of the apatite crystals analyzed (e.g., samples AL08 and FY23; Fig. S2; Flowers et al., 2023). Helium atoms generated within the stopping distance of an alpha particle from the grain margin may be expelled from the crystal, while those produced at the same distance outside of the crystal can be incorporated into the grain through a process known as He implantation (Farley, 2002; Spiegel et al., 2009; Gautheron et al., 2012). Grains with lower eU and He concentrations are particularly vulnerable to biases toward older age estimates, as the injected He significantly influences the overall He budget (e.g., Murray et al., 2014; Janowski et al., 2017; Flowers et al., 2023). After comparing those grains to corresponding AFT ages and other published thermochronological data, we decided not to include the AHe ages of samples AL08 and FY23, which are exceptionally dispersed and anomalously old (Table S2). For the remaining three samples (AL10, FY20, and QH16), after removing the outliers, we were able to obtain geologically meaningful AHe single-grain ages of ca. 162–151 Ma, ca. 101–80 Ma, and ca. 121–70 Ma, with corresponding mean ages of ca. 158 Ma, ca. 88 Ma, and ca. 90 Ma, respectively (Tables 1 and S2).

Thermal History Modeling

Inverse thermal history modeling was performed on data from 23 samples, and the results are divided into four groups based on different localities (Fig. 6). For a more quantitative description of the cooling history, we empirically define the cooling rates of <0.5 °C/Ma, 0.5–2 °C/Ma, and >2 °C/Ma as slow, moderate, and rapid cooling, respectively (e.g., He et al., 2022a, 2023b). Three samples from the marginal area of the southern Altai (the Xibodu region) produced thermal history models that indicate prolonged slow-to-moderate cooling (<1 °C/Ma) during the Mesozoic (Fig. 6A). Among them, the southernmost and oldest (AFT central age) sample, AL12, exhibits a monotonic and prolonged cooling path throughout the entire Mesozoic and Cenozoic, with >100 m.y. of residence time within the apatite partial annealing zone. In the other three study areas (the Altay, Fuyun, and Qinghe regions), the thermal history models of the samples analyzed are highly comparable, and the majority of them show that accelerated rock cooling occurred in the Late Cretaceous (Figs. 6B–6D). These models show initial moderate to rapid cooling (with rates of ~1.5–4 °C/m.y.) to within the temperature window of the apatite partial annealing zone

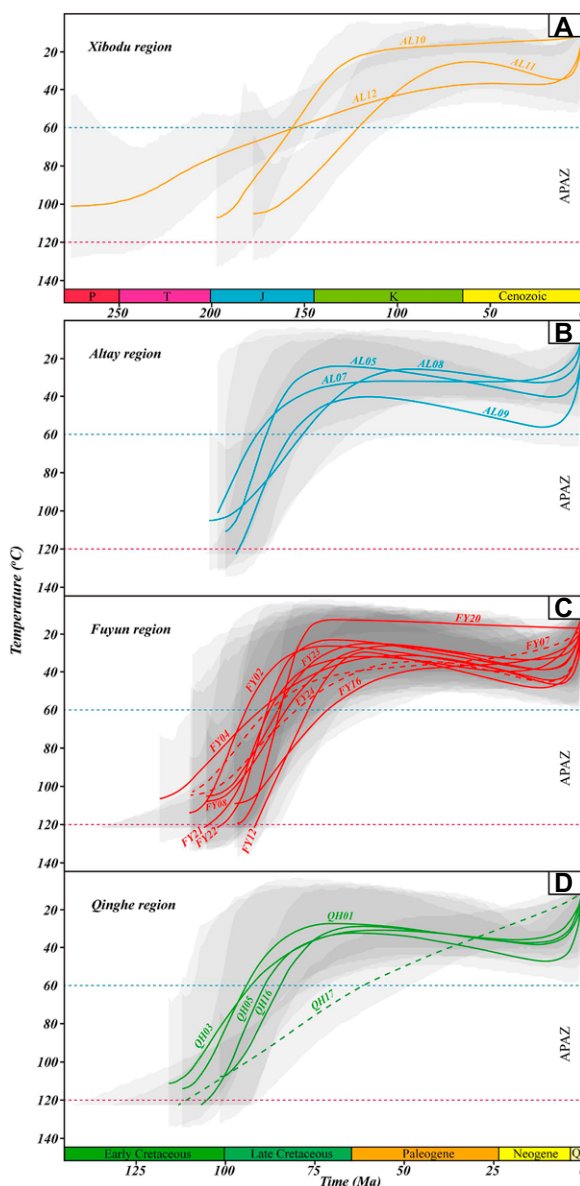


Figure 6. Plot exhibiting the modeled temperature-time paths (“expected” models) with 95% confidence intervals in shadow for the 22 samples analyzed from the southern Altai. Modeling was performed using the QTQt software package (Gallagher, 2012). Cooling curves are grouped based on tectonic units: (A) the Xibodu samples, (B) the Altay samples, (C) the Fuyun samples, and (D) the Qinghe samples. Dashed line shows results from the model that was based on fewer than 50 confined track length measurements. Individual track length histograms and temperature-time plots are provided in Figure S3 (see text footnote 1). APAZ—apatite partial annealing zone; P—Permian; T—Triassic; J—Jurassic; K—Cretaceous.

in the mid-Cretaceous, lasting until the latest Cretaceous, which was then followed by very limited Cenozoic cooling. It is also noted that the slight “re-heating” and subsequent “cooling” observed are possibly due to a modeling artifact that occurs when the software requires a late cooling event to bridge the gap between the present-day surface temperature and the considerably higher temperature required by the model for the observed amount of annealing (e.g., Ketcham et al., 1999; He et al., 2021). The latter typically occurs when the initial track length (l_0) of unannealed induced fission tracks in apatite (~16.3 μm in Durango; Green et al., 1989) overestimates the true initial track length of spontaneous tracks in apatite, which has specific annealing kinetics and a lower initial track length than ~16.3 μm. Considering that these parts of the cooling paths

are completely beyond the apatite partial annealing zone window, they are not further considered to be geologically meaningful. Sample QH17, from the Qinghe region, has exhibited a different and linear cooling path since the mid-Cretaceous (Fig. 6D), but this thermal history model is only based on 48 confined fission-track lengths and, therefore, is less constrained.

DATA INTERPRETATION AND DISCUSSION

AFT and AHe Thermochronological Interpretations

Our samples cover several key areas of the southern Altai, including the Altay, Xibodu, and Fuyun regions at the interface between the

southernmost Altai and the Junggar basin, and the Qinghe region that borders the East Junggar arc (Fig. 1). The new Late Cretaceous AFT ages from the Altay, Fuyun, and Qinghe regions are highly comparable, and the associated confined track lengths generally display narrow and unimodal distributions (Fig. S3), which are indicative of contemporary accelerated cooling through the apatite partial annealing zone. The AHe method is more sensitive to low-temperature perturbations ($<80^{\circ}\text{C}$) than the AFT system, and the AHe ages are therefore expected to be younger than their respective AFT ages. The AHe single-grain ages acquired (excluding outliers) are Late Jurassic to Late Cretaceous, which further corroborates a corresponding Jurassic and Late Cretaceous denudation of the southern Altai crystalline basement. In addition, our AHe dates are in good agreement with the previously reported AHe dataset from the Chinese Altai, in which the AHe single-grain ages are dominantly Cretaceous (Pullen et al., 2020). This indicates that there was no significant Cenozoic exhumation (i.e., less than $\sim 2\text{ km}$) along this orogenic belt. The inverse thermal history models further show that the Late Cretaceous basement cooling (ca. 110–70 Ma; cooling rates of $\sim 1.5\text{--}4^{\circ}\text{C/m.y.}$) was widespread (Fig. 6), and occurred both inside and outside of the inherited and reactivated structures such as ductile shear zones (i.e., the Tuer'hongshate and Irtysh shear zones; Figs. 4 and 5). This suggests that the Late Cretaceous reactivation and deformation in the southern Altai was not only concentrated along major tectonic structures. In addition, samples FY07, FY11, and FY16 were located near the Fuyun fault (Fig. 4), and exhibit Late Cretaceous (ca. 90–75 Ma) AFT ages similar to those of other samples from the Fuyun region, which indicates that the Cenozoic movement of the Fuyun fault did not invoke intensive vertical displacement and denudation of the faulted rocks.

It is noted that a slight Cenozoic reheating is observed in many of the models in all four study areas (Fig. 6). As indicated in the Thermal History Modeling section, it is unclear whether this artifact is a result of the annealing equations or the modeling approach (Vermeesch and Tian, 2014), and independent geological data is, thus, necessary to interpret this type of recurrent time-temperature pattern. In the case of the Cenozoic Altai orogenic belt, it is widely accepted that the continent-continent collision of India and Eurasia in the early Cenozoic, and particularly the ongoing indentation of India into the Eurasia plate, were responsible for the active tectonic processes observed there (e.g., Tapponnier and Molnar, 1979; De Grave and Van den Haute, 2002; Cunningham et al., 2003; De Grave et al.,

2014). In this regard, strain and stress buildup at the collision zone due to continuing convergence was in part released as movements and deformation along inherited zones of lithospheric weakness far into the interior of Eurasia, which resulted in the present-day elevated relief of the Altai Mountain ranges (Cunningham et al., 1996; Buslov et al., 2008). Consequently, our study areas in the southern Altai were not likely to experience subsidence, burial, and heating in the late Cenozoic.

Late Cretaceous and Cenozoic Reactivation of the Southern Altai

Previous low-temperature thermochronological studies have shown that the Altai orogenic belt experienced a phase of significant cooling and exhumation during the Cretaceous, and this has been interpreted to be a far-field effect of strain propagation originating at the Mesozoic distant plate margins (either related to the Mongol-Okhotsk orogen to the east, or tectonic processes at the Tethys margin to the south; De Grave and Van den Haute, 2002; De Grave et al., 2008, 2014; Yuan et al., 2006; Glorie et al., 2012a, 2012b). A recent study of Glorie et al. (2023) and our new AFT and AHe data have further confirmed that the Late Cretaceous (ca. 100–70 Ma) exhumation can be regarded as a regional event that affected much of the southern Altai orogenic belt.

To interpret the AFT data in a wider regional context, a plot of AFT age versus mean track length is presented in Figure 7, based on published AFT data from Yuan et al. (2006) and Glorie et al. (2023) and our new data. This plot demonstrates the relationship between AFT ages and mean track lengths for a series of samples from an area that underwent multistage thermo-tectonic events (Green, 1986; Gallagher and Brown, 1997). In this plot, the Jurassic to Early Cretaceous AFT ages are largely associated with relatively short mean track lengths ($<13\text{ }\mu\text{m}$), which indicates fission-track annealing and long residence time within the apatite partial annealing zone of these analyzed rocks. In the Late Cretaceous (ca. 90–70 Ma), a half “boomerang” begins to curve up toward longer mean track lengths, which is suggestive of a distinct Late Cretaceous cooling event (Fig. 7) in the southern Altai basement. In addition, on the topographic map of the southern Altai and adjacent areas (with indications of available AFT ages and localities), rocks in the higher elevation and relief areas are found to be characterized by younger AFT ages (Late Cretaceous), while those in the flat (i.e., low-relief) areas (indicated in shadow in Fig. 8) largely display older AFT ages (Middle Jurassic to Early Cretaceous). As

a result, the Late Cretaceous reactivation likely built significant relief in the southern Altai.

The cause of the Late Cretaceous reactivation in the southern Altai and other localities of Central Asia has been attributed to the Mongol-Okhotsk orogeny, but its impact on the reactivation of the Central Asian Orogenic Belt structures at that time was probably less significant. During the Late Jurassic and Early Cretaceous, sustained subduction of the Mongol-Okhotsk oceanic plate finally led to complete closure of the oceanic basin, and plutons from the Siberian active margin typically yield crystallization ages from the Triassic to Late Jurassic (Donskaya et al., 2013, and references therein). Collision of the North China craton and the assembled Siberian orogenic margin resulted in the construction of the Mongol-Okhotsk orogenic belt (Xu et al., 2013; Wang et al., 2015, 2022; Zorin, 1999). The collision has been documented by AFT dates that indicate an important Early Cretaceous denudation of the orogen in the Baikal area (Van der Beek et al., 1996). In addition, deformation also reached the Siberian cratonic border in the Transbaikal area (e.g., Zorin, 1999; Jolivet et al., 2009), and the northern margin of the North China craton (e.g., Yang et al., 2015; Dong et al., 2018; Huang et al., 2022). Some previous studies assumed that post-orogenic collapse related to the Mongol-Okhotsk orogeny may have occurred (Jolivet et al., 2009; in Lake Baikal). However, in the Altai orogenic belt, there is no structural evidence for this, such as the occurrence of detachment faults, mylonites, or even high-angle normal faults. Consequently, the Mongol-Okhotsk orogeny largely predated the Late Cretaceous exhumation of the basement in the southern Altai orogenic belt, and dominantly controlled the Mesozoic deformational history of the Mongol-Okhotsk orogenic belt and adjacent areas in East Asia, excluding the southern Altai orogenic belt in Central Asia.

Alternatively, from the Triassic to Cretaceous, the southern margin of the amalgamating Eurasian continent experienced renewed collision of various island arcs and terranes that had rifted from Gondwana and progressively accreted to Eurasia, which led to its reactivation within the Central Asian interior (Dumitru et al., 2001; Glorie and De Grave, 2016; Jepson et al., 2018; He et al., 2022a). During the Early Cretaceous, the Lhasa block gradually collided with Eurasia along the Bangong-Nujiang suture (Kapp et al., 2007; Zhu et al., 2016; Ma et al., 2017), and its far-field effects caused deformation and exhumation in Central Asia, including to the Tianshan orogenic belt and Junggar arcs (e.g., Hendrix et al., 1992; De Grave et al., 2011; De Pelsmaeker et al., 2015; He et al., 2022a, 2022b). In the mid-Cretaceous, subduction of the Neo-

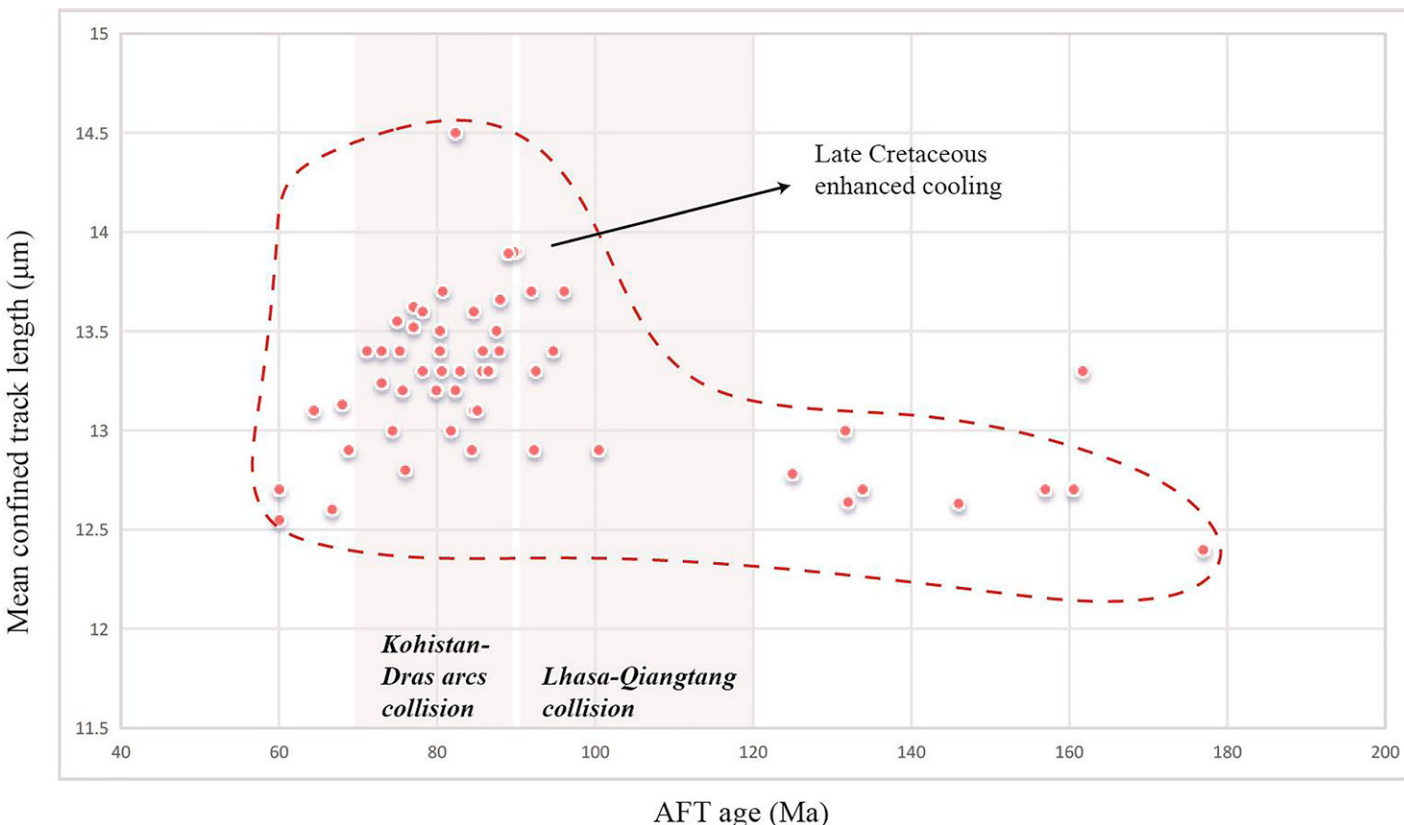


Figure 7. “Boomerang plot” based on the relationship between apatite fission-track (AFT) ages and mean track lengths. This plot highlights a period of prolonged slow cooling during the Jurassic and Early Cretaceous, followed by a cooling pulse in the Late Cretaceous in the southern Altai basement. AFT data are from Yuan et al. (2006), Glorie et al. (2023), and this study.

Tethys oceanic plate continued in the western part of the Eurasian margin, while to the east, the Burmese part of Mega Lhasa accreted completely (Zhu et al., 2013). An island arc system, that is, the Dras–Kohistan–Ladakh arc, collided with the Pamirs and the Lhasa block in the early Late Cretaceous (Fig. 9; Vince and Treolar, 1996; Khan et al., 2009; Jagoutz et al., 2019). This formed the northern suture along which the Himalayas started to develop around the Cretaceous–Paleogene transition, and also caused intense deformation within the Pamirs (Searle et al., 1999; Chapman et al., 2018). Although extensive thermo-tectonic data demonstrate that during the Late Cretaceous and early Paleogene, large parts of the Tianshan and Junggar orogenic collage located south of the Altai orogenic belt experienced tectonic stability and quiescence (Sobel et al., 2006b; Jolivet et al., 2010, 2018), some localized regions experienced continued deformation and exhumation during the mid-to-Late Cretaceous, particularly the central and eastern segments of the Tianshan and the East Junggar, which are adjacent to our study area (e.g., Jolivet et al., 2010; Gillespie et al., 2017; He et al., 2022a). Therefore, we interpret the

Late Cretaceous reactivation of the southern Altai as a response to the far-field effects of the Lhasa–Qiangtang collision and the subsequent accretion of the Dras–Kohistan–Ladakh arc (i.e., Cimmerian collisions; Fig. 9).

While the late Mesozoic thermo-tectonic history of the Altai orogenic belt is well-constrained by low-temperature thermochronology (De Grave and Van den Haute, 2002; Yuan et al., 2006; De Grave et al., 2008; Glorie et al., 2012a, 2023; Pullen et al., 2020; this study), this is not the case for its Cenozoic evolution. The timing of the Cenozoic tectonic reactivation of the Altai Mountain ranges in response to India–Eurasia collision is rather poorly constrained. Paleo-climatic studies suggest that the primary phase of uplift, which shaped the present Altai topography and contributed to the aridification of Central Asia, may be as recent as the late Miocene (e.g., Caves et al., 2014, 2017). This is supported by sedimentological evidence, such as the occurrence of coarse sands and conglomerates within the intramontane basins of the Altai (e.g., the Kurai–Chuya basin; Buslov et al., 1999), as well as structural evidence in terms of Neogene reactivation of preexisting faults (Cunningham

et al., 2003; Cunningham, 2007; Glorie et al., 2012b). In the southern Altai, recent seismic results reveal underthrusting of the lower crust of the East Junggar beneath the southern (Chinese) Altai Mountain ranges, with intracontinental deformation primarily concentrated in the latter due to the existence of a preexisting detachment zone (Yang et al., 2024). As a result, the southern Altai has been prone to more intense and recent Cenozoic deformation. But the Cenozoic reactivation is largely undetected by low-temperature thermochronology (De Grave et al., 2007, 2008, 2009; Glorie et al., 2012a).

Regional Tectonic Significance

The findings of this study align with earlier work in the Altai region of the middle Central Asian Orogenic Belt, yet they provide a significant expansion of the existing dataset. Glorie and De Grave (2016) proposed that upper crustal exhumation in the Altai orogenic belt began during the Jurassic, based on limited AFT data. However, the majority of available low-temperature thermochronological data (AFT and AHe) point to exhumation in the Cretaceous

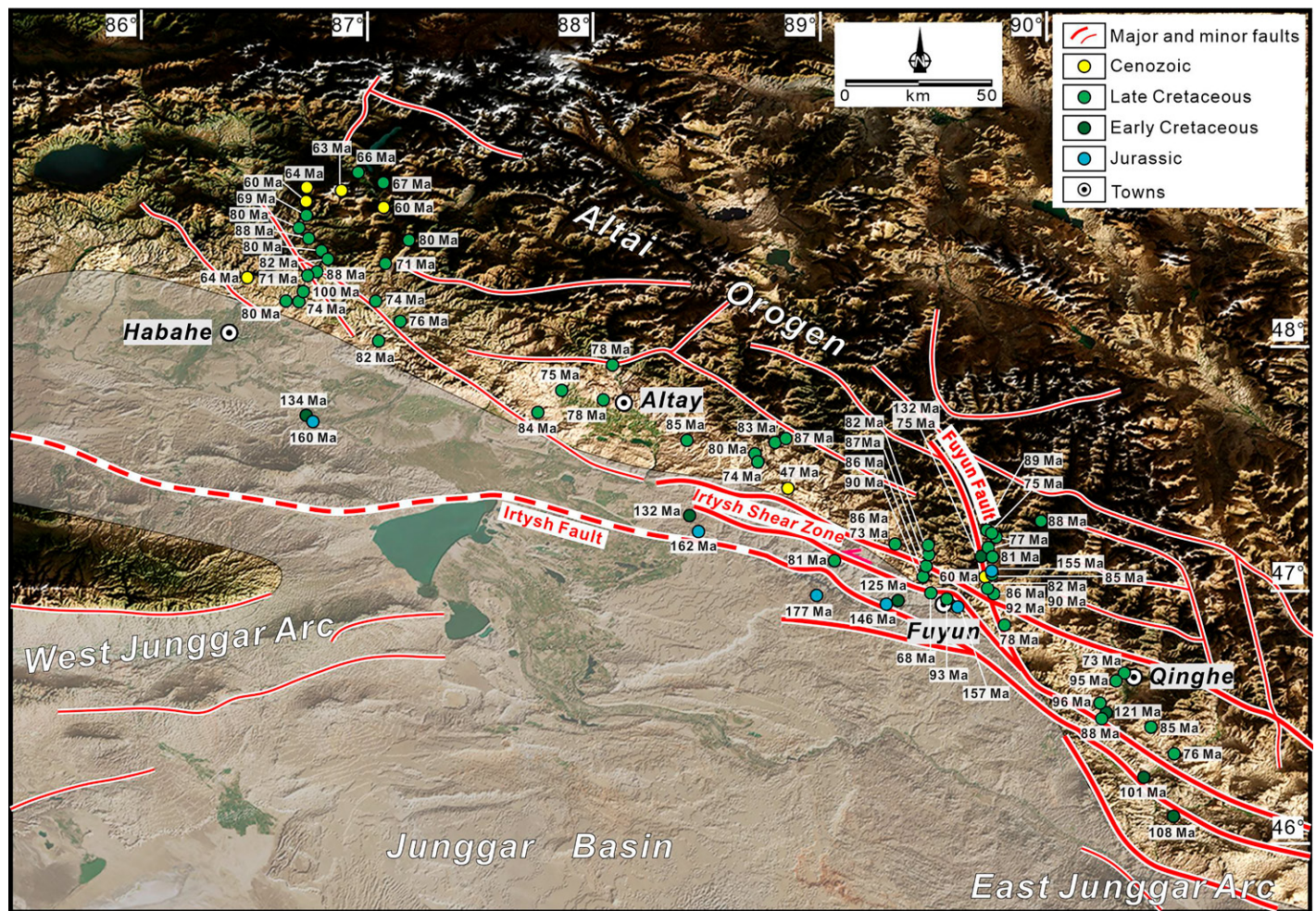


Figure 8. Topographic model of the southern Altai, Central Asia, with present-day structures and newly obtained (this study) and published (Yuan et al., 2006; Pullen et al., 2020; Glorie et al., 2023) apatite fission-track ages. Low-relief (flat) areas are indicated in shadow. Refer to text for detailed discussion.

or earliest Paleogene. Notably, our study fills a critical gap by contributing new thermochronological evidence for exhumation and cooling in the southern Altai, where previous studies identified scarce Cenozoic data. These new data reinforce the hypothesis that much of the current Altai landscape is a remnant of late Mesozoic relief, particularly in areas such as the southern Altai (Fig. 8).

In the northern (Siberian) Altai and western Sayan, AFT data show Late Cretaceous (ca. 95–75 Ma) basement cooling (Glorie et al., 2012a; De Grave et al., 2014), particularly localized along major structures, which suggests a fault-controlled reactivation (Glorie and De Grave, 2016). Our study area in the Altay region remained largely unaffected by the reactivation of fault zones, but the AFT data are very similar (ca. 87–78 Ma; Figs. 6B–6D). This is also the case in the Kanas region to the west of our Altay study area (Yuan et al., 2006). Therefore,

the Late Cretaceous reactivation in the southern Altai was a widespread phenomenon based on thermochronological data, but only a limited thickness of clastic sediments attests to this. Indeed, in the adjacent northern Junggar basin, available field data and seismic profiles reveal that the Upper Cretaceous strata are almost absent (XBGMR, 1993; Li et al., 2015a; He et al., 2022a). An arid climate during this period (Hendrix et al., 1992; Allen and Vincent, 1997; Pullen et al., 2020) may have resulted in limited erosion and the production of detrital sediments. In addition, Li et al. (2023) recently conducted zircon and AFT dating on several Carboniferous to Early Cretaceous sandstones and tuffs (both outcrop rocks and borehole samples) collected from the northern Junggar basin, and identified two Late Cretaceous tectono-thermal events during ca. 93–81 Ma and ca. 72–66 Ma. They proposed that these two events reflect contemporaneous uplift and cooling of the northern Junggar

basin, and linked them to the distant effects of the collision between the Lhasa terrane and the Kohistan-Dras island arc. This further confirms that the Cimmerian collisions' far-field effects triggered considerable regional tectonic events in the interior of Central Asia.

In several parts of Central Asia, the remnants of the inherited Mesozoic landscape features are preserved as uplifted and tectonically dissected peneplanation surfaces with low-relief morphology (e.g., Cunningham et al., 2003). In the Siberian Altai, for example, the uplifted low-relief Chulyshman plateau experienced Late Jurassic to mid-Cretaceous enhanced basement cooling (AFT ages of ca. 130–90 Ma), followed by a Late Cretaceous–early Neogene period of stability characterized by very slow cooling, which was linked to a regional planation (De Grave et al., 2008). Peneplanation surfaces are also common in the Gobi and Mongolian Altai to the east of our study area (Cunningham, 2005,

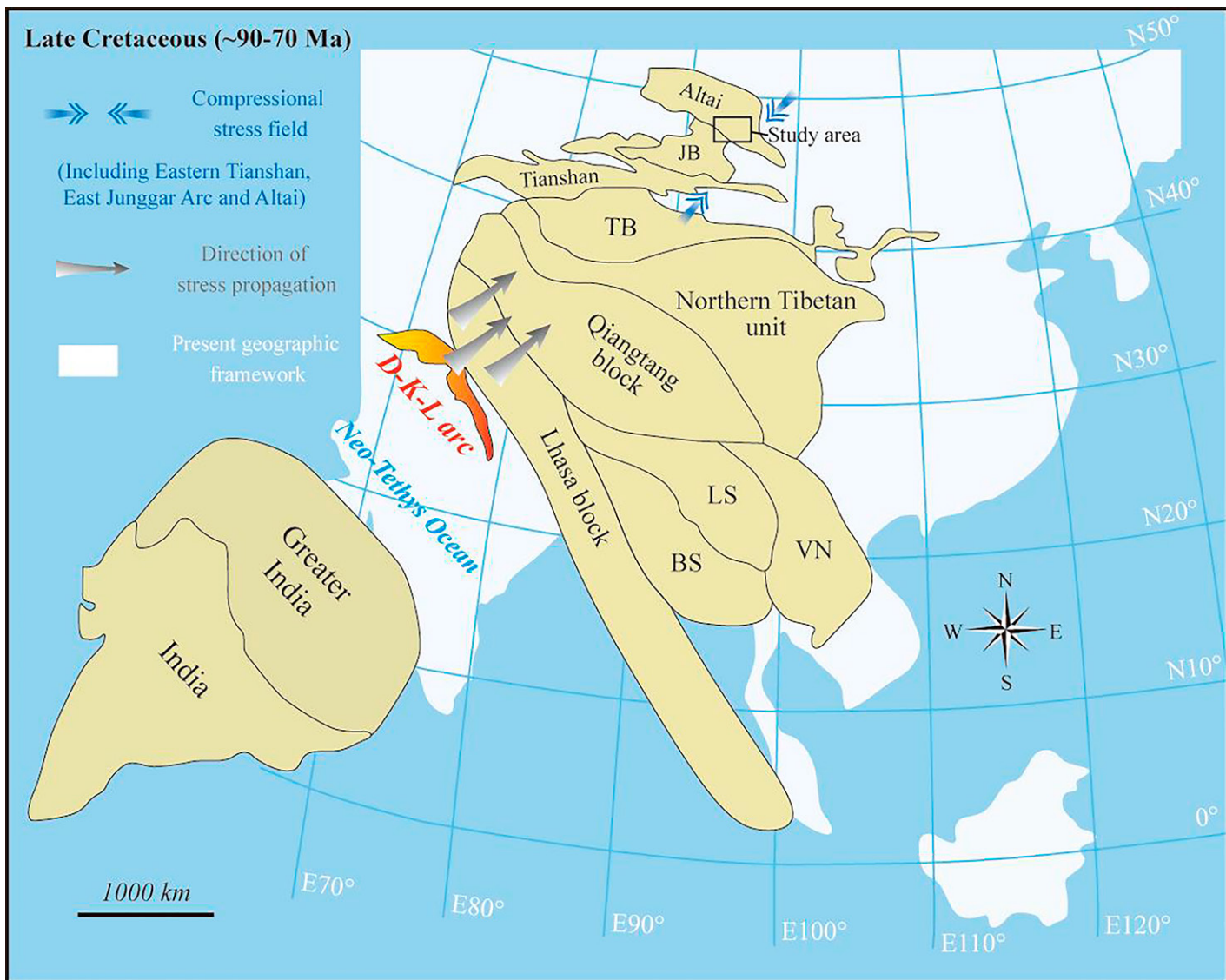


Figure 9. Simplified paleogeographic map of eastern Eurasia in the Late Cretaceous, showing the positions of various continental blocks and oceanic plates. Refer to text for detailed discussion. Tectonic units: BS—Baoshan-Sibumasu unit; D-K-L arc—Dras-Kohistan-Ladakh arc; JB—Junggar basin; LS—Lanping-Simao unit; TB—Tarim basin; VN—Vietnam unit.

2007). Jolivet et al. (2007) provided absolute age constraints on the formation of two elevated (~4000 m in altitude) summit plateaus (i.e., the Baatar massif of the Mongolian Altai and the Ih Bogd massif of the Gobi Altai), and found that these surfaces have persisted for >150 m.y. since the Jurassic, followed by a final uplift in the late Cenozoic. Other available low-temperature thermochronological results also reveal that mountain ranges in the Gobi Altai experienced protracted periods (>100 m.y.) of negligible denudation between the Jurassic and late Cenozoic (Vassallo et al., 2007).

The majority of samples analyzed in this study have also undergone very limited cooling since the latest Cretaceous (Fig. 6). How-

ever, our study areas in the southern Altai do not show such geomorphological features (i.e., typical uplifted or tilted low-relief surfaces; Fig. 8). This can be explained by the hypothesis that more intense Cenozoic reactivation and tectonic uplift occurred to remove these features, but the magnitude of denudation was insufficient to be registered in the low-temperature thermochronological systems at current outcrop levels.

CONCLUSIONS

Drawing on the results of AFT and AHe thermochronology from this study, along with findings from previous research, the following conclusions can be made about the Meso-

Cenozoic thermo-tectonic history of the Altai orogenic belt:

(1) The low-elevation and low-relief Xibodu region in the southern Altai orogenic belt is characterized by relatively old basement rock AFT and AHe ages (ca. 177–132 Ma). This region has experienced slow-to-moderate cooling since the Triassic–Jurassic, and shows some tectonic stability.

(2) Large parts of the southern Altai orogenic belt experienced strong Late Cretaceous reactivation, in response to the far-field effects of the Cimmerian collisions, including the Lhasa-Qiangtang collision in the Early Cretaceous and subsequent accretion of the Dras-Kohistan-Ladakh arc to the southern Eurasian margin.

Distal effects of the Mongol-Okhotsk orogeny were not likely related to the Late Cretaceous deformation in the Altai.

(3) The Late Cretaceous low-temperature thermochronological signals are widely distributed in the western Altai orogenic belt, including the Chinese (southern) and Siberian (northern) Altai. Contemporaneous accelerated basement cooling occurred both inside and outside of the major fault zones in the southern Altai, whereas Late Cretaceous rapid rock cooling in the northern Altai was largely controlled by major structures, with older (e.g., Triassic to Jurassic) cooling ages preserved in the compartments between them.

(4) The present-day southern Altai orogenic belt displays considerable topographic relief, but no Cenozoic AFT or AHe age has been found. Hence, despite the apparent Cenozoic reactivation and deformation in the Altai, denudation seems to have been insufficient to remove the older low-temperature thermochronometric signal.

ACKNOWLEDGMENTS

We appreciate the help provided by Bart Van Houdt and Guido Vittiglio with irradiation at the Belgian Nuclear Research Centre in Mol (SCK-CEN, BR1 facility). Wenbo Su, Ann-Eline Debeer, and Jan Jurceka are thanked for assistance in sample preparation. We thank Science Editor Mihai Dueca for efficient editorial handling, and Jian Chang and Dunfeng Xiang for providing constructive comments that helped to improve the paper. This work is partly funded by the National Key Research and Development Plan of China (grants 2017YFC0601402 and 2018YFC0603703).

REFERENCES CITED

- Allen, M.B., and Vincent, S.J., 1997, Fault reactivation in the Junggar region, Northwest China: The role of basement structures during Mesozoic-Cenozoic compression: *Journal of the Geological Society*, v. 154, p. 151–155, <https://doi.org/10.1144/gjsigs.154.1.0151>.
- Auvouac, J.-P., and Tapponnier, P., 1993, Kinematic model of active deformation in Central Asia: *Geophysical Research Letters*, v. 20, p. 895–898, <https://doi.org/10.1029/93GL00128>.
- Briggs, S.M., Yin, A., Manning, C.E., Chen, Z.-L., Wang, X.-F., and Grove, M., 2007, Late Paleozoic tectonic history of the Ertix fault in the Chinese Altai and its implications for the development of the Central Asian orogenic system: *Geological Society of America Bulletin*, v. 119, p. 944–960, <https://doi.org/10.1130/B26044.1>.
- Brown, R.W., Beucher, R., Roper, S., Persano, C., Stuart, F., and Fitzgerald, P., 2013, Natural age dispersion arising from the analysis of broken crystals. Part I: Theoretical basis and implications for the apatite (UTh)/He thermochronometer: *Geochimica et Cosmochimica Acta*, v. 122, p. 478–497, <https://doi.org/10.1016/j.gca.2013.05.041>.
- Burbank, D.W., and Pinter, N., 1999, Landscape evolution: The interactions of tectonics and surface processes: *Basin Research*, v. 11, p. 1–6, <https://doi.org/10.1046/j.1365-2117.1999.00089.x>.
- Buslov, M.M., Zykin, V.S., Novikov, I.S., and Delvaux, D., 1999, The Cenozoic history of the Chuya depression (Gorny Altai): Structure and geodynamics: *Russian Geology and Geophysics*, v. 40, p. 1687–1701.
- Buslov, M.M., Kokh, D.A., and De Grave, J., 2008, Mesozoic-Cenozoic tectonics and geodynamics of Altai, Tien Shan, and Northern Kazakhstan, from apatite fission-track data: *Russian Geology and Geophysics*, v. 49, p. 648–654, <https://doi.org/10.1016/j.rgg.2008.01.006>.
- Cai, K.D., Sun, M., Yuan, C., Zhao, G.C., Xiao, W.J., Long, X.P., and Wu, F.Y., 2011, Prolonged magmatism, juvenile nature and tectonic evolution of the Chinese Altai, NW China: Evidence from zircon U-Pb and Hf isotopic study of Paleozoic granitoids: *Journal of Asian Earth Sciences*, v. 42, p. 949–968, <https://doi.org/10.1016/j.jseaes.2010.11.020>.
- Cai, K.D., Sun, M., Yuan, C., Xiao, W.J., Zhao, G.C., Long, X.P., and Wu, F.Y., 2012, Carboniferous mantle derived felsic intrusion in the Chinese Altai, NW China: Implications for geodynamic change of the accretionary orogenic belt: *Gondwana Research*, v. 22, p. 681–698, <https://doi.org/10.1016/j.gr.2011.11.008>.
- Carlson, W.D., Donelick, R.A., and Ketcham, R.A., 1999, Variability of apatite fission-track annealing kinetics: I. Experimental results: *The American Mineralogist*, v. 84, p. 1213–1223, <https://doi.org/10.2138/am-1999-0901>.
- Caves, J.K., Sjostrom, D.J., Mix, H.T., Winnick, M.J., and Chamberlain, C.P., 2014, Aridification of Central Asia and uplift of the Altai and Hangay Mountains, Mongolia: Stable isotope evidence: *American Journal of Science*, v. 314, p. 1171–1201, <https://doi.org/10.2475/08.2014.01>.
- Caves, J.K., Bayashashov, B.U., Zhamangara, A., Ritch, A.J., Ibarra, D.E., Sjostrom, D.J., Mix, H.T., Winnick, M.J., and Chamberlain, C.P., 2017, Late Miocene uplift of the Tian Shan and Altai and reorganization of Central Asia climate: *GSA Today*, v. 27, p. 19–26, <https://doi.org/10.1130/GSATG305A.1>.
- Chai, F.M., Mao, J.W., Dong, L.H., Yang, F.Q., Liu, F., Geng, X.X., and Zhang, Z.X., 2009, Geochronology of metarhyolites from the Kangbutiebao Formation in the Kelang basin, Altay Mountains, Xinjiang: Implications for the tectonic evolution and metallogeny: *Gondwana Research*, v. 16, p. 189–200, <https://doi.org/10.1016/j.gr.2009.03.002>.
- Chapman, J.B., Robinson, A.C., Carrapa, B., Villarreal, D., Worthington, J., DeCelles, P.G., Kapp, P., Gadoev, M., Oimahmadov, I., and Gehrels, G., 2018, Cretaceous shortening and exhumation history of the South Pamir terrane: *Lithosphere*, v. 10, p. 494–511, <https://doi.org/10.1130/L691.1>.
- Chen, B., and Jahn, B.-M., 2002, Geochemical and isotopic studies of the sedimentary and granitic rocks of the Altai orogen of Northwest China and their tectonic implications: *Geological Magazine*, v. 139, p. 1–13, <https://doi.org/10.1017/S0016756801006100>.
- Cunningham, D., 2005, Active intracontinental transpressional mountain building in the Mongolian Altai: Defining a new class of orogen: *Earth and Planetary Science Letters*, v. 240, p. 436–444, <https://doi.org/10.1016/j.epsl.2005.09.013>.
- Cunningham, D., 2007, Structural and topographic characteristics of restraining bend mountain ranges of the Altai, Gobi Altai and easternmost Tien Shan, in Cunningham, W.D., and Mann, P., eds., *Tectonics of Strike-Slip Restraining and Releasing Bends*: Geological Society, London, Special Publication 290, p. 219–237, <https://doi.org/10.1144/SP290.7>.
- Cunningham, D., 2010, Tectonic setting and structural evolution of the late Cenozoic Gobi Altai orogen, in Kusky, T.M., Zhai, M.G., Xiao, W., eds., *The Evolving Continents: Understanding Processes of Continental Growth*: Geological Society, London, Special Publication 338, p. 361–387, <https://doi.org/10.1144/SP338.17>.
- Cunningham, D., Windley, B.F., Dorjnamjaa, D., Badamgarov, J., and Saandar, M., 1996, Late Cenozoic transpression in southwestern Mongolia and the Gobi Altai-Tien Shan connection: *Earth and Planetary Science Letters*, v. 140, p. 67–81, [https://doi.org/10.1016/0012-821X\(96\)00048-9](https://doi.org/10.1016/0012-821X(96)00048-9).
- Cunningham, D., Owen, L.A., Snee, L.W., and Li, J.L., 2003, Structural framework of a major intracontinental orogenic termination zone: The easternmost Tien Shan, China: *Journal of the Geological Society*, v. 160, p. 575–590, <https://doi.org/10.1144/0016-764902-122>.
- De Grave, J., and Van den Haute, P., 2002, Denudation and cooling of the Lake Teletskoye region in the Altai Mountains (South Siberia) as revealed by apatite fission-track thermochronology: *Tectonophysics*, v. 349, p. 145–159, [https://doi.org/10.1016/S0040-1951\(02\)00051-3](https://doi.org/10.1016/S0040-1951(02)00051-3).
- De Grave, J., Buslov, M.M., and Van den Haute, P., 2007, Distant effects of India-Eurasia convergence and Mesozoic intracontinental deformation in Central Asia: Constraints from apatite fission-track thermochronology: *Journal of Asian Earth Sciences*, v. 29, p. 188–204, <https://doi.org/10.1016/j.jseaes.2006.03.001>.
- De Grave, J., Van den Haute, P., Buslov, M.M., Dehandschutter, B., and Glorie, S., 2008, Apatite fission-track thermochronology applied to the Chulyshman plateau, Siberian Altai region: *Radiation Measurements*, v. 43, p. 38–42, <https://doi.org/10.1016/j.radmeas.2007.11.068>.
- De Grave, J., Buslov, M.M., Van den Haute, P., Metcalf, J., Dehandschutter, B., and McWilliams, M.O., 2009, Multi-Method chronometry of the Teletskoye graben and its basement, Siberian Altai Mountains: New insights on its thermo-tectonic evolution: *Geological Society, London, Special Publication* 324, p. 237–259, <https://doi.org/10.1144/SP324.17>.
- De Grave, J., Glorie, S., Buslov, M.M., Izmer, A., Fournier-Carrie, A., Batalev, V.Y., Vanhaecke, F., Elburg, M.A., and Van den Haute, P., 2011, The thermo-tectonic history of the Song-Kul plateau, Kyrgyz Tien Shan: Constraints by apatite and titanite thermochronometry and zircon U/Pb dating: *Gondwana Research*, v. 20, p. 745–763, <https://doi.org/10.1016/j.gr.2011.03.011>.
- De Grave, J., De Pelsmaeker, E., Zhimulev, F.I., Glorie, S., Buslov, M.M., and Van den Haute, P., 2014, Meso-Cenozoic building of the northern Central Asian Orogenic Belt: Thermotectonic history of the Tuva region: *Tectonophysics*, v. 621, p. 44–59, <https://doi.org/10.1016/j.tecto.2014.01.039>.
- De Pelsmaeker, E., Glorie, S., Buslov, M.M., Zhimulev, F.I., Poujol, M., Korobkin, V.V., Vanhaecke, F., Vetrov, E.V., and De Grave, J., 2015, Late-Paleozoic emplacement and Meso-Cenozoic reactivation of the southern Kazakhstan granitoid basement: *Tectonophysics*, v. 662, p. 416–433, <https://doi.org/10.1016/j.tecto.2015.06.014>.
- Donelick, R., O'Sullivan, P., and Ketcham, R., 2005, Apatite fission-track analysis: *Reviews in Mineralogy and Geochemistry*, v. 58, p. 49–94, <https://doi.org/10.2138/rmg.2005.58.3>.
- Dong, S.W., Zhang, Y.Q., Li, H.L., Shi, W., Xue, H.M., Li, J.H., Huang, S.Q., and Wang, Y.C., 2018, The Yanshan orogeny and late Mesozoic multi-plate convergence in East Asia—Commemorating 90 years of the “Yanshan Orogeny”: *Science China Earth Sciences*, v. 61, p. 1888–1909, <https://doi.org/10.1007/s11430-017-9297-y>.
- Donskaya, T.V., Gladkochub, D.P., Mazukabzov, A.M., and Ivanov, A.V., 2013, Late Paleozoic–Mesozoic subduction-related magmatism at the southern margin of the Siberian continent and the 150 million-year history of the Mongol-Okhotsk Ocean: *Journal of Asian Earth Sciences*, v. 62, p. 79–97, <https://doi.org/10.1016/j.jseaes.2012.07.023>.
- Dumitru, T.A., Zhou, D., Chang, E.Z., and Graham, S.A., 2001, Uplift, exhumation, and deformation in the Chinese Tien Shan, in Hendrix, M.S., and Davis, G.A., eds., *Paleozoic and Mesozoic Tectonic Evolution of Central and Eastern Asia: From Continental Assembly to Intracontinental Deformation*: Geological Society of America Memoir 194, p. 71–99, <https://doi.org/10.1130/0-8137-1194-0.71>.
- Ehlers, T.A., Farley, K.A., 2003, Apatite (U-Th)/He thermochronometry: Methods and applications to problems in tectonic and surface processes: *Earth and Planetary Science Letters*, v. 206, p. 1–14, [https://doi.org/10.1016/S0012-821X\(02\)01069-5](https://doi.org/10.1016/S0012-821X(02)01069-5).
- Farley, K.A., 2002, (U-Th)/He dating: Techniques, calibrations, and applications, in Porcelli, D., Ballentine, C.J., and Wieler, R., eds., *Noble Gases in Geochemistry and Cosmochemistry*: Berlin, Germany, Walter de Gruyter, *Reviews in Mineralogy and Geochemistry*, v. 47, p. 819–846, <https://doi.org/10.1515/9781509056-020>.
- Fitzgerald, P.G., Baldwin, S.L., Webb, L.E., and O'Sullivan, P.B., 2006, Interpretation of (U-Th)/He single grain

- ages from slowly cooled crustal terranes: A case study from the Transantarctic Mountains of southern Victoria Land: *Chemical Geology*, v. 225, p. 91–120, <https://doi.org/10.1016/j.chemgeo.2005.09.001>.
- Flowers, R.M., Ketcham, R.A., Shuster, D.L., and Farley, K.A., 2009, Apatite (U-Th)/He thermochronometry using a radiation damage accumulation and annealing model: *Geochimica et Cosmochimica Acta*, v. 73, p. 2347–2365, <https://doi.org/10.1016/j.gca.2009.01.015>.
- Flowers, R.M., Ketcham, R.A., Enkelmann, E., Gautheron, C., Reiners, P.W., Metcalf, J.R., Danišk, M., Stockli, D.F., and Brown, R.W., 2023, (U-Th)/He chronology: Part 2. Considerations for evaluating, integrating, and interpreting conventional individual aliquot data: *Geological Society of America Bulletin*, v. 135, p. 137–161, <https://doi.org/10.1130/B36268.1>.
- Galbraith, R.F., and Green, P.F., 1990, Estimating the component ages in a finite mixture: *International Journal of Radiation Applications and Instrumentation. Part D: Nuclear Tracks and Radiation Measurements*, v. 17, p. 197–206, [https://doi.org/10.1016/1359-0189\(90\)90035-V](https://doi.org/10.1016/1359-0189(90)90035-V).
- Gallagher, K., 2012, Transdimensional inverse thermal history modeling for quantitative thermochronology: *Journal of Geophysical Research: Solid Earth*, v. 117, <https://doi.org/10.1029/2011JB008825>.
- Gallagher, K., and Brown, R., 1997, The onshore record of passive margin evolution: *Journal of the Geological Society*, v. 154, p. 451–457, <https://doi.org/10.1144/gsjgs.154.3.0451>.
- Gallagher, K., Charvin, K., Nielsen, S., Sambridge, M., and Stephenson, J., 2009, Markov chain Monte Carlo (MCMC) sampling methods to determine optimal models, model resolution and model choice for Earth Science problems: *Marine and Petroleum Geology*, v. 26, p. 525–535, <https://doi.org/10.1016/j.marpetgeo.2009.01.003>.
- Gautheron, C., Tassan-Got, L., Ketcham, R.A., and Dobson, K.J., 2012, Accounting for long alpha-particle stopping distances in (U-Th-Sm)/He geochronology: 3-D modeling of diffusion, zoning, implantation, and abrasion: *Geochimica et Cosmochimica Acta*, v. 96, p. 44–56, <https://doi.org/10.1016/j.gca.2012.08.016>.
- Gillespie, J., Glorie, S., Jepson, G., Zhang, Z.Y., Xiao, W.J., Danišk, M., and Collins, A.S., 2017, Differential exhumation and crustal tilting in the easternmost Tianshan (Xinjiang, China), revealed by low-temperature thermochronology: *Tectonics*, v. 36, p. 2142–2158, <https://doi.org/10.1002/2017TC004574>.
- Glorie, S., 2012, Chronology of formation and reactivation of the Kyrgyz Tien Shan, Siberian-Kazakh Altai and Kuznetsk Altai basement architecture: Insights from multiple U-decay chronometers [Ph.D. thesis]: Ghent, Belgium, Ghent University, 407 p.
- Glorie, S., and De Grave, J., 2016, Exhuming the Meso-Cenozoic Kyrgyz Tianshan and Siberian Altai-Sayan: A review based on low-temperature thermochronology: *Geoscience Frontiers*, v. 7, p. 155–170, <https://doi.org/10.1016/j.gsf.2015.04.003>.
- Glorie, S., De Grave, J., Buslov, M.M., Elburg, M.A., Stockli, D.F., Gerdes, A., and Van den Haute, P., 2010, Multi-method chronometric constraints on the evolution of the Northern Kyrgyz Tien Shan granitoids (Central Asian Orogenic Belt): From emplacement to exhumation: *Journal of Asian Earth Sciences*, v. 38, p. 131–146, <https://doi.org/10.1016/j.jseas.2009.12.009>.
- Glorie, S., De Grave, J., Buslov, M.M., Zhimulev, F.I., Elburg, M.A., and Van den Haute, P., 2012a, Structural control on Meso-Cenozoic tectonic reactivation and denudation in the Siberian Altai: Insights from multi-method thermochronometry: *Tectonophysics*, v. 544–545, p. 75–92, <https://doi.org/10.1016/j.tecto.2012.03.035>.
- Glorie, S., De Grave, J., Delvaux, D., Buslov, M.M., Zhimulev, F.I., Vanhaecke, F., Elburg, M.A., and Van den Haute, P., 2012b, Tectonic history of the Irtish shear zone (NE Kazakhstan): New constraints from zircon U/Pb dating, apatite fission track dating and paleostress analysis: *Journal of Asian Earth Sciences*, v. 45, p. 138–149, <https://doi.org/10.1016/j.jseas.2011.09.024>.
- Glorie, S., Nixon, A.L., Jepson, G., Gillespie, J., Warren, C., Meeuws, F., Simpson, A., and Xiao, W.J., 2023, Meso-Cenozoic tectonic history of the Altai: New insights from apatite U-Pb and fission track thermochronology for the Fuyun area (Xinjiang, China): *Tectonics*, v. 42, <https://doi.org/10.1029/2022TC007692>.
- Green, P.F., 1986, On the thermo-tectonic evolution of Northern England: Evidence from fission track analysis: *Geological Magazine*, v. 123, p. 493–506, <https://doi.org/10.1017/S0016756800035081>.
- Green, P.F., Duddy, I.R., Laslett, G.M., Hegarty, K.A., Gleadow, A.J.W., and Lovering, J.F., 1989, Thermal annealing of fission tracks in apatite 4. Quantitative modelling techniques and extension to geological timescales: *Chemical Geology: Isotope Geoscience Section*, v. 79, p. 155–182, [https://doi.org/10.1016/0168-9622\(89\)90018-3](https://doi.org/10.1016/0168-9622(89)90018-3).
- Guenther, W.R., Reiners, P.W., Ketcham, R.A., Nasdala, L., and Giester, G., 2013, Helium diffusion in natural zircon: Radiation damage, anisotropy, and the interpretation of zircon (U-Th)/He thermochronology: *American Journal of Science*, v. 313, p. 145–198, <https://doi.org/10.2475/03.2013.01>.
- He, Z.Y., 2022, Intra-continental evolution of the Chinese Tianshan and Junggar orogenic collage [Ph.D. thesis]: Ghent, Belgium, Ghent University, 276 p.
- He, Z.Y., Wang, B., Nachtergaelie, S., Glorie, S., Ni, X.H., Su, W.B., Cai, D.X., Liu, J.S., and De Grave, J., 2021, Long-term topographic evolution of the Central Tianshan (NW China) constrained by low-temperature thermochronology: *Tectonophysics*, v. 817, <https://doi.org/10.1016/j.tecto.2021.229066>.
- He, Z.Y., Wang, B., Glorie, S., Su, W.B., Ni, X.H., Jepson, G., Liu, J.S., Zhong, L.L., Gillespie, J., and De Grave, J., 2022a, Mesozoic building of the Eastern Tianshan and East Junggar (NW China) revealed by low-temperature thermochronology: *Gondwana Research*, v. 103, p. 37–53, <https://doi.org/10.1016/j.gr.2021.11.013>.
- He, Z.Y., Wang, B., Su, W.B., Glorie, S., Ni, X.H., Liu, J.S., Cai, D.X., Zhong, L.L., and De Grave, J., 2022b, Meso-Cenozoic thermo-tectonic evolution of the Yili block within the Central Asian Orogenic Belt (NW China): Insights from apatite fission track thermochronology: *Tectonophysics*, v. 823, <https://doi.org/10.1016/j.tecto.2021.229194>.
- He, Z.Y., Zhong, L.L., Su, W.B., Zhong, K.H., Glorie, S., Ren, F., Shen, X.M., Song, S.D., Dou, J., Qin, Q., and De Grave, J., 2023a, Low-temperature thermochronology of the Longmalala-Mengya's Pb-Zn deposits (southern Tibet): Implications for ore exhumation and preservation: *Ore Geology Reviews*, v. 160, <https://doi.org/10.1016/j.oregeorev.2023.105611>.
- He, Z.Y., Glorie, S., Wang, F.J., Zhu, W.B., Fonseca, A., Su, W.B., Zhong, L.L., Zhu, X., and De Grave, J., 2023b, A re-evaluation of the Meso-Cenozoic thermo-tectonic evolution of Bogda Shan (Tian Shan, NW China) based on new basement and detrital apatite fission track thermochronology: *International Geology Review*, v. 65, p. 2093–2112, <https://doi.org/10.1080/00206814.2022.2121946>.
- Hendrix, M.S., Graham, S.A., Carroll, A.R., Sobel, E.R., McKnight, C.L., Schulein, B.J., and Wang, Z.X., 1992, Sedimentary record and climatic implications of recurrent deformation in the Tian Shan: Evidence from Mesozoic strata of the North Tarim, South Junggar, and Turpan basins, Northwest China: *Geological Society of America Bulletin*, v. 104, p. 53–79, [https://doi.org/10.1130/0016-7606\(1992\)104<0053:SRACIO>2.3.CO;2](https://doi.org/10.1130/0016-7606(1992)104<0053:SRACIO>2.3.CO;2).
- Holdsworth, R.E., Butler, C.A., and Roberts, A.M., 1997, The recognition of reactivation during continental deformation: *Journal of the Geological Society*, v. 154, p. 73–78, <https://doi.org/10.1144/gsjgs.154.1.0073>.
- Hu, W.W., Li, P.F., Rosenbaum, G., Liu, J.L., Jourdan, F., Jiang, Y.D., Wu, D., Zhang, J., Yuan, C., and Sun, M., 2020, Structural evolution of the eastern segment of the Irtish shear zone: Implications for the collision between the East Junggar terrane and the Chinese Altai orogen (northwestern China): *Journal of Structural Geology*, v. 139, <https://doi.org/10.1016/j.jsg.2020.104126>.
- Huang, S.-Q., Dong, S.-W., Zhang, F., Zhang, Y.-Q., Shi, W., and Müller, W.E.G., 2022, Timing of the Kaiyuan-Jiapigou shear zone in the northern margin of the North China craton: Implications for closure of the Mongolian Ocean: *Tectonophysics*, v. 844, <https://doi.org/10.1016/j.tecto.2022.229626>.
- Jagoutz, O., Bouilhol, P., Schaltegger, U., and Müntener, O., 2019, The isotopic evolution of the Kohistan Ladakh arc from subduction initiation to continent arc collision, in Treloar, P.J., and Searle, M.P., eds., *Himalayan Tectonics: A Modern Synthesis*: Geological Society, London, Special Publication 483, p. 165–182, <https://doi.org/10.1144/SP483.7>.
- Jahn, B.-M., 2004, The Central Asian Orogenic Belt and growth of the continental crust in the Phanerozoic, in Malpas, J., et al., eds., *Aspects of the Tectonic Evolution of China*: Geological Society, London, Special Publication 226, p. 73–100, <https://doi.org/10.1144/GSL.SP.2004.226.01.05>.
- Janowski, M., Loget, N., Gautheron, C., Barbarand, J., Bellahsen, N., Van den Driessche, J., Babault, J., and Meyer, B., 2017, Neogene exhumation and relief evolution in the eastern Betics (SE Spain): Insights from the Sierra de Gador: *Terra Nova*, v. 29, p. 91–97, <https://doi.org/10.1111/ter.12252>.
- Jepson, G., Glorie, S., Konopelko, D., Gillespie, J., Danisik, M., Mirkalalov, R., Mamadjanov, Y., and Collins, A.S., 2018, Low-temperature thermochronology of the Chatkal-Kurama terrane (Uzbekistan-Tajikistan): Insights into the Meso-Cenozoic thermal history of the western Tian Shan: *Tectonics*, v. 37, p. 3954–3969, <https://doi.org/10.1029/2017TC004878>.
- Jiang, Y.D., Sun, M., Zhao, G.C., Yuan, C., Xiao, W.J., Xia, X.P., Long, X.P., and Wu, F.Y., 2011, Precambrian detrital zircons in the early Paleozoic Chinese Altai: Their provenance and implications for the crustal growth of Central Asia: *Precambrian Research*, v. 189, p. 140–154, <https://doi.org/10.1016/j.precamres.2011.05.008>.
- Jiang, Y.D., Schulmann, K., Sun, M., Štípká, P., Guy, A., Janoušek, V., Lexa, O., and Yuan, C., 2016, Anatexis of accretionary wedge, Pacific-type magmatism, and formation of vertically stratified continental crust in the Altai orogenic belt: *Tectonics*, v. 35, p. 3095–3118, <https://doi.org/10.1029/2016TC004271>.
- Jolivet, M., Ritz, J.F., Vassallo, R., Larroque, C., Braucher, R., Todileg, M., Chauvet, A., Sue, C., Arnaud, N., De Vicente, R., Arzhanikova, A., and Arzhanikov, S., 2007, Mongolian summits: An uplifted, flat, old but still preserved erosion surface: *Geology*, v. 35, p. 871–874, <https://doi.org/10.1130/G23758A.1>.
- Jolivet, M., Boisrrollier, T., Petit, C., Fournier, M., Sankov, V.A., Ringenbach, J.-C., Bykov, L., Miroshnichenko, A.I., Kovalenko, S.N., and Anisimova, S.V., 2009, How old is the Baikal Rift Zone? Insight from apatite fission track thermochronology: *Tectonics*, v. 28, <https://doi.org/10.1029/2008TC002404>.
- Jolivet, M., Dominguez, S., Charreau, J., Chen, Y., Li, Y., and Wang, Q., 2010, Mesozoic and Cenozoic tectonic history of the central Chinese Tian Shan: Reactivated tectonic structures and active deformation: *Tectonics*, v. 29, <https://doi.org/10.1029/2010TC002712>.
- Jolivet, M., Heilbronn, G., Robin, C., Barrier, L., Bourquin, S., Guo, Z., Jia, Y., Guerit, L., Yang, W., and Fu, B., 2013, Reconstructing the Late Palaeozoic–Mesozoic topographic evolution of the Chinese Tian Shan: Available data and remaining uncertainties: *Advances in Geosciences*, v. 37, p. 7–18, <https://doi.org/10.5194/ageo-37-7-2013>.
- Jolivet, M., Barrier, L., Dauteuil, O., Laborde, A., Li, Q., Reichenbacher, B., Popescu, S.-M., Sha, J., and Guo, Z., 2018, Late Cretaceous–Palaeogene topography of the Chinese Tian Shan: New insights from geomorphology and sedimentology: *Earth and Planetary Science Letters*, v. 499, p. 95–106, <https://doi.org/10.1016/j.epsl.2018.07.004>.
- Käbner, A., Ratschbacher, L., Pfänder, J.A., Hacker, B.R., Zack, G., Sonntag, B.L., Khan, J., Stanek, K.P., Gadeov, M., and Oimahmadov, I., 2017, Proterozoic–Mesozoic history of the Central Asian orogenic belt in the Tajik and southwestern Kyrgyz Tian Shan: U-Pb, $^{40}\text{Ar}/^{39}\text{Ar}$, and fission-track geochronology and geochemistry of granitoids: *Geological Society of America Bulletin*, v. 129, p. 281–303, <https://doi.org/10.1130/B31466.1>.
- Kapp, P., DeCelles, P.G., Gehrels, G.E., Heizler, M., and Ding, L., 2007, Geological records of the Lhasa-Qiangtang and Indo-Asian collisions in the Nima area of

- Central Tibet: Geological Society of America Bulletin, v. 119, p. 917–933, <https://doi.org/10.1130/B26033.1>.
- Ketcham, R.A., Donelick, R.A., and Carlson, W.D., 1999, Variability of apatite fission-track annealing kinetics: III. Extrapolation to geological time scales: The American Mineralogist, v. 84, p. 1235–1255, <https://doi.org/10.2138/am-1999-0903>.
- Ketcham, R.A., Carter, A., Donelick, R.A., Barbarand, J., and Hurford, A.J., 2007, Improved modeling of fission-track annealing in apatite: The American Mineralogist, v. 92, p. 799–810, <https://doi.org/10.2138/am.2007.2281>.
- Khan, S.D., Walker, D.J., Hall, S.A., Burke, K.C., Shah, M.T., and Stockli, L., 2009, Did the Kohistan-Ladakh island arc collide first with India?: Geological Society of America Bulletin, v. 121, p. 366–384, <https://doi.org/10.1130/B26348.1>.
- Klinger, Y., Etchebes, M., Tapponnier, P., and Narteau, C., 2011, Characteristic slip for five great earthquakes along the Fuyun fault in China: Nature Geoscience, v. 4, p. 389–392, <https://doi.org/10.1038/ngeo1158>.
- Kong, X.Y., Zhang, C., Liu, D.D., Jiang, S., Luo, Q., Zeng, J.H., Liu, L.F., Luo, L., Shao, H.B., Liu, D., Liu, X.Y., and Wang, X.P., 2019, Disequilibrium partial melting of metasediments in subduction zones: Evidence from O-Nd-Hf isotopes and trace elements in S-type granites of the Chinese Altai: Lithosphere, v. 11, p. 149–168, <https://doi.org/10.1130/L1039.1>.
- Laurent-Charvet, S., Charvet, J., Monié, P., and Shu, L.S., 2003, Late Paleozoic strike-slip shear zones in eastern Central Asia (NW China): New structural and geochronological data: Tectonics, v. 22, no. 2, <https://doi.org/10.1029/2001TC001047>.
- Li, D., He, D.F., Santosh, M., Ma, D.L., and Tang, J.Y., 2015a, Tectonic framework of the northern Junggar basin part I: The eastern Luliang uplift and its link with the East Junggar terrane: Gondwana Research, v. 27, p. 1089–1109, <https://doi.org/10.1016/j.gr.2014.08.015>.
- Li, P., Sun, M., Rosenbaum, G., Cai, K., Chen, M., and He, Y., 2016, Transpressional deformation, strain partitioning and fold superimposition in the southern Chinese Altai, Central Asian orogenic belt: Journal of Structural Geology, v. 87, p. 64–80, <https://doi.org/10.1016/j.jsg.2016.04.006>.
- Li, P.F., Sun, M., Rosenbaum, G., Cai, K.D., and Yu, Y., 2015b, Structural evolution of the Irtysh Shear Zone (northwestern China) and implications for the amalgamation of arc systems in the Central Asian Orogenic Belt: Journal of Structural Geology, v. 80, p. 142–156, <https://doi.org/10.1016/j.jsg.2015.08.008>.
- Li, P.F., Sun, M., Rosenbaum, G., Jourdan, F., Li, S.Z., and Cai, K.D., 2017, Late Paleozoic closure of the Ob-Zaisan Ocean along the Irtysh shear zone (NW China): Implications for arc amalgamation and oroclinal bending in the Central Asian orogenic belt: Geological Society of America Bulletin, v. 129, p. 547–569, <https://doi.org/10.1130/B31541.1>.
- Li, Z.H., Chen, Z.J., Fan, Y.H., Yu, L., Zhang, S.Y., and Li, X.Y., 2023, Fission-track thermochronological evidence for the Yanshanian tectonic evolution of the northern Junggar basin, Northwest China: Frontiers of Earth Science, v. 11, <https://doi.org/10.3389/feart.2023.1023655>.
- Lin, Z.F., Yuan, C., Zhang, Y.Y., Sun, M., Long, X.P., Wang, X.Y., Huang, Z.Y., and Chen, Z.W., 2019, Petrogenesis and geodynamic implications of two episodes of Permian and Triassic high-silica granitoids in the Chinese Altai, Central Asian Orogenic Belt: Journal of Asian Earth Sciences, v. 184, <https://doi.org/10.1016/j.jseaes.2019.103978>.
- Liu, W., Liu, L.J., Liu, X.J., Shang, H.J., and Zhou, G., 2010, Age of the Early Devonian Kangbutiebao Formation along the southern Altay Mountains and its northeastern extension: Acta Petrologica Sinica (Yanshi Xuebao), v. 26, p. 387–400 [in Chinese with English abstract].
- Liu, W., Liu, X.J., and Xiao, W.J., 2012, Massive granitoid production without massive continental-crust growth in the Chinese Altay: Insight into the source rock of granitoids using integrated zircon U-Pb age, Hf-Nd-Sr isotopes and geochemistry: American Journal of Science, v. 312, p. 629–684, <https://doi.org/10.2475/06.2012.02>.
- Long, X.P., Sun, M., Yuan, C., Xiao, W.J., Lin, S.F., Wu, F.Y., Xia, X.P., and Cai, K.D., 2007, Detrital zircon age and Hf isotopic studies for metasedimentary rocks from the Chinese Altai: Implications for the early Paleozoic tectonic evolution of the Central Asian Orogenic Belt: Tectonics, v. 26, <https://doi.org/10.1029/2007TC002128>.
- Ma, A.L., Hu, X.M., Garzanti, E., Han, Z., and Lai, W., 2017, Sedimentary and tectonic evolution of the southern Qiangtang basin: Implications for the Lhasa-Qiangtang collision timing: Journal of Geophysical Research: Solid Earth, v. 122, p. 4790–4813, <https://doi.org/10.1002/2017JB014211>.
- Morin, J., Jolivet, M., Robin, C., Heilbronn, G., Barrier, L., Bourquin, S., and Jia, Y., 2018, Jurassic paleogeography of the Tian Shan: An evolution driven by far-field tectonics and climate: Earth-Science Reviews, v. 187, p. 286–313, <https://doi.org/10.1016/j.earscirev.2018.10.007>.
- Murray, K.E., Orme, D.A., and Reiners, P.W., 2014, Effects of U-Th-rich grain boundary phases on apatite helium ages: Chemical Geology, v. 390, p. 135–151, <https://doi.org/10.1016/j.chemgeo.2014.09.023>.
- Pullen, A., Banaszynski, M., Kapp, P., Thomson, S.N., and Cai, F.L., 2020, A mid-Cretaceous change from fast to slow exhumation of the western Chinese Altai Mountains: A climate driven exhumation signal?: Journal of Asian Earth Sciences, v. 197, <https://doi.org/10.1016/j.jseas.2020.104387>.
- Raimondo, T., Hand, M., and Collins, W.J., 2014, Compresional intracontinental orogens: Ancient and modern perspectives: Earth-Science Reviews, v. 130, p. 128–153, <https://doi.org/10.1016/j.earscirev.2013.11.009>.
- Searle, M.P., Khan, M.A., Fraser, J.E., Gough, S.J., and Jan, M.Q., 1999, The tectonic evolution of the Kohistan-Karakoram collision belt along the Karakoram highway transect, North Pakistan: Tectonics, v. 18, p. 929–949, <https://doi.org/10.1029/1999TC000042>.
- Shen, X.M., Zhang, H.X., Wang, Q., Wyman, D.A., and Yang, Y.H., 2011, Late Devonian–Early Permian A-type granites in the southern Altay Range, Northwest China: Petrogenesis and implications for tectonic setting of “A2-type” granites: Journal of Asian Earth Sciences, v. 42, p. 986–1007, <https://doi.org/10.1016/j.jseas.2010.10.004>.
- Shen, X.M., Tian, Y.T., Zhang, G.H., Zhang, S.M., Carter, A., Kohn, B., Vermeesch, P., Liu, R., and Li, W., 2019, Late Miocene hinterland crustal shortening in the Longmen Shan thrust belt, the eastern margin of the Tibetan plateau: Journal of Geophysical Research: Solid Earth, v. 124, p. 11,972–11,991, <https://doi.org/10.1029/2019JB018358>.
- Sobel, E.R., Chen, J., and Heermance, R.V., 2006a, Late Oligocene–early Miocene initiation of shortening in the Southwestern Chinese Tian Shan: Implications for Neogene shortening rate variations: Earth and Planetary Science Letters, v. 247, p. 70–81, <https://doi.org/10.1016/j.epsl.2006.03.048>.
- Sobel, E.R., Oskin, M., Burbank, D., and Mikolaichuk, A., 2006b, Exhumation of basement-cored uplifts: Example of the Kyrgyz Range quantified with apatite fission track thermochronology: Tectonics, v. 25, <https://doi.org/10.1029/2005TC001809>.
- Spiegel, C., Kohn, B., Belton, D., Berner, Z., and Gleadow, A., 2009, Apatite (U-Th-Sm)/He thermochronology of rapidly cooled samples: The effect of He implantation: Earth and Planetary Science Letters, v. 285, p. 105–114, <https://doi.org/10.1016/j.epsl.2009.05.045>.
- Sun, M., Yuan, C., Xiao, W.J., Long, X.P., Xia, X.P., Zhao, G.C., Lin, S.F., Wu, F.Y., and Kröner, A., 2008, Zircon U-Pb and Hf isotopic study of gneissic rocks from the Chinese Altai: Progressive accretionary history in the early to middle Palaeozoic: Chemical Geology, v. 247, p. 352–383, <https://doi.org/10.1016/j.chemgeo.2007.10.026>.
- Tapponnier, P., and Molnar, P., 1979, Active faulting and Cenozoic tectonics of the Tien Shan, Mongolia, and Baykal regions: Journal of Geophysical Research: Solid Earth, v. 84, p. 3425–3459, <https://doi.org/10.1029/JB084iB07p03425>.
- Tong, Y., Hong, D.W., Wang, T., Wang, S.G., and Han, B.F., 2006, TIMS U-Pb zircon ages of Fuyun post-orogenic linear granite plutons on the southern margin of Altay orogenic belt and their implications: Acta Petrologica et Mineralogica, v. 25, p. 85–89 [in Chinese with English abstract].
- Tong, Y., Wang, T., Jahn, B.-m., Sun, M., Hong, D.-W., and Gao, J.-F., 2014, Post-accretionary Permian granitoids in the Chinese Altai orogen: Geochronology, petrogenesis and tectonic implications: American Journal of Science, v. 314, p. 80–109, <https://doi.org/10.2475/01.2014.03>.
- Van der Beek, P.A., Delvaux, D., Andriessen, P.A.M., and Levi, K.G., 1996, Early Cretaceous denudation related to convergent tectonics in the Baikal region, SE Siberia: Journal of the Geological Society, v. 153, p. 515–523, <https://doi.org/10.1144/gsjgs.153.4.0515>.
- Vassallo, R., Jolivet, M., Ritz, J.-F., Braucher, R., Larroque, C., Sue, C., Todileg, M., and Javkhlanbold, D., 2007, Uplift age and rates of the Gurvan Bogd system (Gobi-Altay) by apatite fission track analysis: Earth and Planetary Science Letters, v. 259, p. 333–346, <https://doi.org/10.1016/j.epsl.2007.04.047>.
- Vermeesch, P., and Tian, Y.T., 2014, Thermal history modeling: HeFTy vs. QTQt: Earth-Science Reviews, v. 139, p. 279–290, <https://doi.org/10.1016/j.earscirev.2014.09.010>.
- Vince, K.J., and Treloar, P.J., 1996, Miocene, north-vergent extensional displacements along the Main Mantle Thrust, NW Himalaya, Pakistan: Journal of the Geological Society, v. 153, p. 677–680, <https://doi.org/10.1144/gsjgs.153.5.0677>.
- Wagner, G.A., and Van den Haute, P., 1992, Fission Track-Dating: Dordrecht, Netherlands, Kluwer Academic Publishers, 285 p., <https://doi.org/10.1007/978-94-0112478-2>.
- Wang, T., Jahn, B.-M., Kovach, V.P., Tong, Y., Hong, D.-W., and Han, B.-F., 2009, Nd-Sr isotopic mapping of the Chinese Altai and implications for continental growth in the Central Asian Orogenic Belt: Lithos, v. 110, p. 359–372, <https://doi.org/10.1016/j.lithos.2009.02.001>.
- Wang, T., Guo, L., Zhang, L., Yang, Q.D., Zhang, J.J., Tong, Y., and Ye, K., 2015, Timing and evolution of Jurasico-Cretaceous granitoid magmatisms in the Mongol-Okhotsk belt and adjacent areas, NE Asia: Implications for transition from contractional crustal thickening to extensional thinning and geodynamic settings: Journal of Asian Earth Sciences, v. 97, p. 365–392, <https://doi.org/10.1016/j.jseas.2014.10.005>.
- Wang, T., Tong, Y., Xiao, W.J., Guo, L., Windley, B.F., Donskaya, T., Li, S., Tserendash, N., and Zhang, J.J., 2022, Rollback, scissor-like closure of the Mongol-Okhotsk Ocean and formation of an orocline: Magmatic migration based on a large archive of age data: National Science Review, v. 9, <https://doi.org/10.1093/nsr/nwab210>.
- Windley, B.F., Kröner, A., Guo, J.H., Qu, G.S., Li, Y.Y., and Zhang, C., 2002, Neoproterozoic to Paleozoic geology of the Altai orogen, NW China: New zircon age data and tectonic evolution: The Journal of Geology, v. 110, p. 719–737, <https://doi.org/10.1086/342866>.
- Windley, B.F., Alexeev, D., Xiao, W.J., Kröner, A., and Bardach, G., 2007, Tectonic models for accretion of the Central Asian Orogenic Belt: Journal of the Geological Society, v. 164, p. 31–47, <https://doi.org/10.1144/0016-7649-2006-022>.
- Whipple, K., 2009, The influence of climate on the tectonic evolution of mountain belts: Nature Geoscience, v. 2, p. 97–104, <https://doi.org/10.1038/ngeo413>.
- Wolf, R.A., Farley, K.A., and Kass, D.M., 1998, Modeling of the temperature sensitivity of the apatite (U-Th)/He thermochronometer: Chemical Geology, v. 148, p. 105–114, [https://doi.org/10.1016/S0009-2541\(98\)00024-2](https://doi.org/10.1016/S0009-2541(98)00024-2).
- Wu, C., Huang, K., Yin, A., Zhang, J.Y., Zuza, A.Z., Haproff, P.J., and Ding, L., 2024, Tectonic geomorphology and Quaternary slip history of the Fuyun fault, southwestern Altai Mountains, Central Asia: Geosphere, v. 20, p. 735–748, <https://doi.org/10.1130/GES02737.1>.
- XBGMR (Xinjiang Bureau of Geology and Mineral Resources), 1965, Geological map, Er'Tai sheet (L-46-XIII): Xinjiang Bureau of Geology and Mineral Resources, scale 1:200,000.
- XBGMR (Xinjiang Bureau of Geology and Mineral Resources), 1978a, Geological map, Altay sheet (L-45-V): Xinjiang Bureau of Geology and Mineral Resources, scale 1:200,000.

- XBGMR (Xinjiang Bureau of Geology and Mineral Resources), 1978b, Geological map, Xibudu sheet (L-45-XI): Xinjiang Bureau of Geology and Mineral Resources, scale 1:200,000.
- XBGMR (Xinjiang Bureau of Geology and Mineral Resources), 1978c, Geological map, Fuyun sheet (L-45-XII): Xinjiang Bureau of Geology and Mineral Resources, scale 1:200,000.
- XBGMR (Xinjiang Bureau of Geology and Mineral Resources), 1993, Regional Geology of Xinjiang Uygur Autonomy Region: Beijing, Geological Publishing House, 841 p. [in Chinese].
- Xu, W.-L., Pei, F.-P., Wang, F., Meng, E., Ji, W.-Q., Yang, D.-B., and Wang, W., 2013, Spatial-temporal relationships of Mesozoic volcanic rocks in NE China: Constraints on tectonic overprinting and transformations between multiple tectonic regimes: *Journal of Asian Earth Sciences*, v. 74, p. 167–193, <https://doi.org/10.1016/j.jseaes.2013.04.003>.
- Yang, X.S., Tian, X.B., Wan, B., Yuan, H.Y., Zhao, L., and Xiao, W.J., 2024, Impact of ancient tectonics on intracontinental deformation partitioning: Insights from crustal structures of the East Junggar-Alтай area: *Journal of Geophysical Research: Solid Earth*, v. 129, <https://doi.org/10.1029/2023JB027949>.
- Yang, Y.T., Guo, Z.X., Song, C.C., Li, X.B., and He, S., 2015, A short-lived but significant Mongol-Okhotsk collisional orogeny in latest Jurassic-earliest Cretaceous: *Gondwana Research*, v. 28, p. 1096–1116, <https://doi.org/10.1016/j.gr.2014.09.010>.
- Yuan, C., Sun, M., Xiao, W.J., Li, X.H., Chen, H.L., Lin, S.F., Xia, X.P., and Long, X.P., 2007, Accretionary orogenesis of the Chinese Altai: Insights from Paleozoic granitoids: *Chemical Geology*, v. 242, p. 22–39, <https://doi.org/10.1016/j.chemgeo.2007.02.013>.
- Yuan, W.M., Carter, A., Dong, J.Q., Bao, Z.K., An, Y.C., and Guo, Z.J., 2006, Mesozoic-Tertiary exhumation history of the Altai Mountains, northern Xinjiang, China: New constraints from apatite fission track data: *Tectonophysics*, v. 412, p. 183–193, <https://doi.org/10.1016/j.tecto.2005.09.007>.
- Zhang, C.L., Santosh, M., Zou, H.B., Xu, Y.G., Zhou, G., Dong, Y.G., Ding, R.F., and Wang, H.Y., 2012, Revisiting the “Irish tectonic belt”: Implications for the Paleozoic tectonic evolution of the Altai orogen: *Journal of Asian Earth Sciences*, v. 52, p. 117–133, <https://doi.org/10.1016/j.jseas.2012.02.016>.
- Zhu, D.C., Zhao, Z.D., Niu, Y.L., Dilek, Y., Hou, Z.Q., and Mo, X.X., 2013, The origin and pre-Cenozoic evolution of the Tibetan plateau: *Gondwana Research*, v. 23, p. 1429–1454, <https://doi.org/10.1016/j.gr.2012.02.002>.
- Zhu, D.C., Li, S.M., Cawood, P., Wang, Q., Zhao, Z.D., Liu, S.A., and Wang, L.Q., 2016, Assembly of the Lhasa and Qiangtang terranes in central Tibet by divergent double subduction: *Lithos*, v. 245, p. 7–17, <https://doi.org/10.1016/j.lithos.2015.06.023>.
- Zorin, Y.A., 1999, Geodynamics of the western part of the Mongolia-Okhotsk collisional belt, Trans-Baikal region (Russia) and Mongolia: *Tectonophysics*, v. 306, p. 33–56, [https://doi.org/10.1016/S0040-1951\(99\)00042-6](https://doi.org/10.1016/S0040-1951(99)00042-6).

SCIENCE EDITOR: MIHAI DUCEA

ASSOCIATE EDITOR: DONGFANG SONG

MANUSCRIPT RECEIVED 19 JULY 2024

REVISED MANUSCRIPT RECEIVED 9 NOVEMBER 2024

MANUSCRIPT ACCEPTED 2 DECEMBER 2024